Novel *N*-Chloramine Based Antibacterial and Non-adherent Burn Wound Dressings

by

Chenxi Ning

A Thesis Submitted to the Faculty of Graduate Studies of
the University of Manitoba
in Partial Fulfilment of the Requirements of the Degree of

MASTER OF SCIENCE

Department of Textile Sciences
University of Manitoba
Winnipeg, Manitoba

TABLE OF CONTENTS

ACKNOWLEDGEMENTS

I would like to thank Dr. Song Liu for his support as chair of my committee. His trust and faith in my abilities made me successfully finish this Master program in two years. I am fortunate to have had such a dedicated supervisor who worked with me, providing his scientific advice, invaluable guidance, and consistent patience throughout the process.

I would like to thank my committee members Dr. Sarvesh Logsetty and Dr. Ayush Kumar for their time and insightful comments on my thesis. Special thanks are extended to Dr. Logsetty for providing me medical materials and beneficial suggestion on adherence measurement in accordance with his abundant experience in clinical burn care; Dr. Kumar for his kind help with antibacterial tests and results analysis; Dr. Lingdong Li and Mr. Sadegh Ghanbar for their efforts in organic synthesis of novel biocides used in this study; Dr. Shivkumar Ghugare for his instructions in polymerization and characterization of hydrogels; Dr. Wajihah Mughal for her training in cell culture. This project would not have been possible without their generous assistance and support.

I am also grateful for the financial support from the University of Manitoba Graduate Fellowship (UMGF), the Manitoba Graduate Scholarship (MGS), the Collaborative Health Research Projects (CHRP) operating grant (Grant no.: CHRP 413713 2012) and the Natural Sciences and Engineering Research Council (NSERC) of Canada Discovery grant (Grant no.: RGPIN/372048 2009).

Finally, I would like to acknowledge the Medical Textile Surface Engineering lab members and my parents who supported me, taught me, and shared their knowledge and experience with me

ABSTRACT

A burn is a type of injury to the skin caused by fire, heat, electricity, chemicals, radiation or friction. It occurs in all age groups. Burn wound infection remains the leading cause of skin graft failure and one of the leading causes of burn injury related mortality. Dressings impregnated with silver compounds are the mainstay of treatment for burn wounds to prevent or combat the infection. However, most commercially available silver based wound dressings cause trauma upon removal because of adhesion to the wound bed. A recent study has shown that burn dressing related pain is linked to more severe depressive and posttraumatic stress symptoms. Furthermore, emerging resistance associated with silver based wound dressings is a growing concern. Organic *N*-chloramines (*N*-chloro-derivatives of amines and amides) have been in clinical use for over 180 years thanks to their effectiveness toward a broad spectrum of microorganisms, and no resistance has been yet reported. *N*-chloramines possess oxidative potential and attack multi-targets in bacteria such as thiols and amines in proteins, which is the reason for the absence of the development of bacterial resistance. This study aimed to develop an "ideal" wound dressing with both antibacterial and non-adherent properties. Poly(ethylene terephthalate) (PET) fabrics are among the most representative base materials in burn wound dressings (ActicoatTM and Atrauman®) and thus were chosen as the substrate to impart with antibacterial and non-adherent properties. Specifically, a thin layer of polyacrylamide (PAm) hydrogel was deposited onto the surface of PET fabric via plasma activation and photopolymerization. The treated PET fabric (termed as "PET-PAm") was characterized with attenuated total reflectance Fourier transform infrared (ATR-FTIR) spectroscopy and water contact angle measurement. We adapted an *in vitro* wet-gelatin adherence model to evaluate the effect of hydrogel deposition on reducing the adherence of PET. The deposited hydrogel layer was found to lower the adherence of PET fabrics.

The peeling energy of PET decreased drastically from 2231.5 J/m^2 to nearly 250 J/m^2 after the deposition of hydrogel. On the other hand, we have also synthesized a series of new "composite" biocides with both *N*-chloramine and quaternary ammonium (QA) moieties. Those "composite" biocides exert boosted killing efficiency against methicillin-resistant *Staphylococcus aureus* (MRSA) and multi-drug resistant (MDR) *Pseudomonas aeruginosa*. Increasing the alkyl chain length of QA moiety resulted in an increase in the antibacterial activity of these "composite" compounds. A synergistic effect was detected against MRSA. The deposited hydrogel layer can also serve as the reservoir for the loading of the novel *N*-chloramine based "composite" biocides. Two "composite" compounds with long alkyl chain, as well as their corresponding precursors, were loaded into the hydrogel deposited PET fabrics via a swelling method, followed by *in vitro* release studies in phosphate-buffered saline (PBS, 0.1 M, pH 7.4). "Composite" compounds showed a higher loading capacity compared to long-chained QA salts alone, which was due to the transchlorination from *N*-chloramide to PAm hydrogel, resulting in the promotion in the uptake of biocides. All the biocides achieved approximately 90% of release within 540 min. Overall, this study demonstrated the potential of coating commonly used dressing materials with PAm hydrogel to both serve as a reservoir for potent *N*-chloramine biocides, and decrease dressing adherence to wounds.

LIST OF ABBREVIATIONS

Concepts:

ASTM	American Society for Testing and Materials
CFU	colony-forming unit
MVTR	moisture vapor transmission rate
RH	relative humidity
RND	resistance-nodulation-division

Chemicals and materials:

AM	acrylamide
CMC	carboxymethylcellulose
CI	cadexomer iodine
DMSO	dimethyl sulfoxide
DI water	deionized water
DMH	5,5-dimethyl hydantoin
DNA	deoxyribonucleic acid
I_2	iodine
KI	potassium iodide
MBA	N,N'-methylene bisacrylamide
MTT	3-(4,5-dimethylthiazol-2-yl)-2,5-diphenyltetrazolium bromide
NaCl	sodium chloride
$Na_2S_2O_3$	sodium thiosulfate
PTFE	polytetrafluoroethylene
PET	poly(ethylene terephthalate)
PAm	polyacrylamide
PET-PAm	polyacrylamide hydrogel deposited on PET dressings
PBS	phosphate-buffered saline
PEG	polyethylene glycol

PVP-I	povidone iodine
QA salts	quaternary ammonium salts

Microbiology:

CA-MRSA	community-associated methicillin-resistant *Staphylococcus aureus*
CT_{50}	cytotoxicity at which 50% of cells survive
MRSA	methicillin-resistant *Staphylococcus aureus*
MDR *P. aeruginosa*	multi-drug resistant *Pseudomonas aeruginosa*
MIC	minimal inhibitory concentration

Instrumentation:

ATR-FTIR	attenuated total reflectance – fourier transform infrared spectroscopy
^{1}H NMR	proton nuclear magnetic resonance
UV	ultraviolet-visible spectroscopy

LIST OF SCHEMES

LIST OF TABLES

LIST OF FIGURES

CHAPTER 1. INTRODUCTION

1.1 Burns

Burns are among the most devastating of all injuries, producing overwhelming physiologic and psychologic impairments.[1-3] Most of burns involve thermal damage such as scalding and fires, while the minority occurs when exposed to ultraviolet radiation, radioactivity, chemicals or electricity.[4-5] Globally in 2004, 11 million people with burn injuries were brought to medical attention, accounting for over 300,000 deaths.[6] Studies demonstrate that there is an age-adjusted rate in the patients with burn injuries, and children particularly those in the 0-4 age group have the highest incidence due to their impulsiveness and unawareness.[5, 7-8] Babies and young children have thin, sensitive skin that develop burns four times quickly and deeply than an adult at the same condition.[9] The highest incidence of hospitalised paediatric burns is in Africa with an incidence rate of 0.0108, as compared to the lowest of 0.0044 of the Americas.[4, 10-1] But over half of the world's paediatric burn population resides in Asia due to Asia's considerably larger population, with 288,560 of burns per year.[10] During the years 1994 to 2003, 10,229 Canadian children aged 0 to 19 years were admitted to hospital because of burn-related injury, of which nearly 5% lost their life.[12] Fortunately, a decline in burn hospitalisations among children has been noted in Canada.

After admission to a burn care, the wound bed must be cleaned with soap and water; all blisters should be left intact to minimise the risk of infection while larger blisters should be aspirated under aseptic technique. Burns can only be managed after a direct visualization of the wound bed to assess the extent and depth. Most burns are relatively small and thus not life-threatening, but large burns still pose a major threat if treated improperly. Even small burns may cause major morbidity due to the significant pain and disfiguring scar formatting.[13]

Burns are stratified into 4 degrees with increasing depth.[1, 13-5] First-degree (superficial) burn is typically the sun burn, affecting the epidermis only and causing erythema without blistering. The skin is usually red, and painful. Second-degree burn, also called partial-thickness burn, can be categorised as either superficial or deep burn. A superficial partial-thickness burn involves the epidermis and the papillary dermis, characterized by local redness, blisters. It heals spontaneously in 5-21 days. Deep partial-thickness burns extend into the reticular dermis, characterized by pain and whiteness. It takes several weeks (21-35 days) to heal without skin grafting, but leaves significant hypertrophic scarring, contraction, and loss of function. Third-degree (full-thickness) burns destroy the entire epidermis and dermis, and may involve the subcutaneous tissue. The wound surface is dry and leather-like to touch. This type of burn will need excision and skin grafting to heal, because all skin appendages are burned away and it can heal only by contraction or migration of keratinocytes from the periphery of the wound. In fourth-degree burns, the entire skin is destroyed and substantial damage goes deeply into the subcutaneous tissue such as muscle, fascia, or bone.[16-7]

However, it is difficult to judge the initial burn depth sometimes, since most large burns are a mixture of different depths. Moreover, the depth of a burn can change and deepen following initial injury. Superficial and partial thickness burns can progress to a deeper burn due to the wound desiccation or wound infection. If a superficial partial-thickness burn takes more than 2 weeks to heal, secondary tangential excision and skin grafting might be necessary.[14] Therefore, appropriate care plays a very important role in the prevention of conversion and thus the improvement of healing rate of burns.

1.2 Burn wound dressing.

Wound dressings have been widely used in burn management to clean, cover and protect the wound from the external environment. Traditional dressings, such as cotton gauzes or bandages, represent the most conventional products used for the treatment of burns, providing a protective barrier to micro-organisms. They also afford other advantages such as good drainage, conformability, and easy use with topical pharmaceuticals. However, these dressing materials have a high tendency to dry out resulting in a dehydrated wound bed, which might inhibit the healing process. Moreover, they adhere to wounds by exudate soaking into dressing fibres and hardening, causing significant pain and trauma to fragile epithelial tissue upon removal.[18-9]

In recognition of these problems, a myriad of modern dressings have been developed as a result of the improvement of technology in conjunction with the better understanding of the wound healing process. They are able to optimize patient local and systemic conditions, and provide an ideal wound healing environment by removing excess exudate, maintaining high humidity at the dressing-wound interface, minimizing tissue trauma upon removal, protecting against bacterial contamination and so on. It is almost impossible to define any one of them as the "gold standard". According to a worldwide online survey among 121 burn care specialists from 39 countries, 49.6% ranked a "non-adherent, non-traumatic wound interface" as the most important characteristic of an "ideal" burn wound dressing, while antimicrobial activity was identified as another key property.[20] Currently, there emerges a series of wound dressings claimed to be antibacterial and non-adherent, such as Silvercel non-adherent antimicrobial alginate, Aquacel Ag antimicrobial hydrofiber, and Mepilex® Ag. Unfortunately, these dressings are not looked upon favorably by most of burn care providers for one reason or another. The development of such a dressing perfectly meeting both expectations still remains a big challenge for researchers.

1.2.1 Infection control.

Infection is a major complication of burns. Most deaths of burn patients today result from infections rather than burns themselves, about 75% of the mortality following burn injuries being related to infections.[21] The skin barrier to microbes is destroyed with burns and replaced by a moist, protein-rich, avascular eschar that fosters microbial growth. Furthermore, infectious complications might be introduced by severe dysfunction of immune system, a large colonization on human skin, the probability of gastrointestinal bacterial translocation, a prolonged hospitalization, and invasive operation in diagnose and medical treatment.[21-3] Although all burned patients were cleaned thoroughly and applied with topical agents (silver sulphadiazine), Macedo[22] found that the microbial colonization in burn wounds still existed in 86.6% of patients at the end of the first week after admission to hospital. The burn wound is colonized predominantly with Gram-positive organisms in the first week, which are fairly quickly replaced by Gram-negative organisms in the subsequent weeks.[24-7] Most of the isolates show high level resistance and thus require treatment with high-efficient, broad-spectrum antimicrobial agents. Gram-negative organisms are the primary cause of serious infection in burn patients in North America, owing to the great motility and various antibiotic resistance mechanisms. They have been associated with a 50% increase in predicted mortality for infected patients.[28] Gram-positive *Staphylococcus aureus* and Gram-negative *Pseudomonas aeruginosa* have become the most frequently isolated organisms in most burn units.[22]

The use of topical antimicrobial therapy has long been fundamental to treat burns. Widespread application in the topical use of effective antimicrobial agents reduces the microbial load on the burn wound surface and lowers the risk of infection. Topical antimicrobials have traditionally been formulated as liquid (solutions, suspensions, and emulsions) and semi-solid (ointments and creams). Solutions such as povidone-iodine (PVP-I) solution are most effective in the initial stage

of wound healing for reducing bacterial load. PVP-I is active against a wide variety of bacteria, fungi, protozoa, and viruses due to the iodination and oxidisation of available iodine in the complex.[29-30] It is also used as a debriding and sloughing agent to remove necrotic tissue from the wound bed. Thymol and hydrogen peroxide are also favorable in wound cleansing and debridement, along with germicidal actions.[31] However, the major problem with liquids is the short residence time on the wound site, especially where there is a considerable amount of exudate. In comparison, semi-solid formulations tend to remain for a longer period of time and exert a more stable antibacterial activity, but they are not very effective at remaining on the area of highly exuding wound as they rapidly absorb liquid, lose their rheological characteristics and become mobile.[32]

New technologies incorporate antimicrobials into modern dressings, such as hydrocolloids, hydrogels, alginates, polyurethane foams/films, and silicone gels, allowing controlled release at the wound surface. Controlled release wound dressings can offer many benefits, such as improvement of the temporal and spatial presentation of active agents on wound sites, protection of antimicrobials against physiological degradation or elimination, increase of bactericidal efficacy compared to the intensity of side effects, and enhancement of patient compliance without frequent dressing change.[33-6] Specifically, the disinfectants incorporated in dressings play the pivotal part in preventing or combating burn infections, which can be categorised into two major groups: antibiotics and antiseptics.

The discovery of antibiotics is one of the most impressive innovations in the previous century, saving innumerable lives. Antibiotics are produced either naturally or synthetically to treat infections caused by bacteria and certain parasites. They usually act on specific cellular targets and have a narrow spectrum of activity. Some kill the bacteria by interfering with the structure of the

cell wall of the bacteria, while some prevent the bacteria from multiplying. However, some highly potent antibiotics are no longer as effective as before, as pathogens can develop resistance to all different classes of antibiotics discovered to date.[37-9] Antibiotic resistance has become a major global healthcare crisis in the 21st century, not only due to the increased number of hospital acquired infections, but also because of the severe infections that are difficult to diagnose and treat. The mechanisms of antibiotic resistance include modification of the target, enzymatic neutralisation of the agent, and inaccessibility of target through reductions in cellular permeability or by prevention the agent from reaching an intracellular target by efflux pump.[37] The emergency of resistance has been mainly attributed to the widespread availability, misuse and overuse of antibiotics in outpatient clinics, hospitalized patients and in the food industry. Thus, those applications where antibiotics are used topically to treat bacterial infections should be minimized.

The use of antiseptics for topical and hard-surface applications has provided a possible solution to the development of antibiotic resistance. Antiseptics are disinfectants that destroy or inhibit the growth of microorganisms on intact skin and some open wounds. They often have multiple microbial targets and a broader antimicrobial spectrum in comparison with antibiotics. Some common types of active chemical agents used in antiseptic products for incorporating into dressings to achieve a controlled release are summarized as follows.

1.2.1.1 Iodine.

Iodine-based products have been used in wound care for more than 150 years without selecting resistant strains in microorganisms.[39] Molecular iodine (I_2) exhibits extensive deleterious effects against bacteria, fungi and viruses. It freely and rapidly penetrates microorganisms, denatures proteins and enzymes by binding to thiol and sulfohydryl groups, and alters phospholipid membrane structures by blocking hydrogen bonding, leading to rapid inactivation of cells.[53, 150]

Early products were commonly prepared in aqueous or alcoholic solutions, causing pain, irritation and excessive staining. To overcome these clinical limitations, iodophors ("iodine carriers" or "iodine-releasing agents") have been developed. They are complexes of molecular iodine or triiodide and a solubilizing agent or carrier, which act as reservoirs of free iodine.[151-2] Povidone iodine (PVP-I) and cadexomer iodine (CI, Iodosorb, Smith and Nephew) are the most well-known iodophors, available in several formulations including solutions, creams and impregnated dressings. Numerous publications describe the use of iodine as a topical agent to prevent or treat localised wound infections, but controversy surrounds not only its efficiency but also the safety for the use in wound care. One of the dangers of topical application of iodine is that iodine can be absorbed through large wounds or during prolonged usage, which might translate to a potential risk of metabolic and toxic complications. There was evidence that absorption of PVP-I gave rise to severe metabolic acidosis in two burns patients and accelerated their death.[153] Iodine is also contraindicated in patients with iodine hypersensitivity and thyroid pathosis to decrease the risk of hypothyroidism.[154]

1.2.1.2 Triclosan.

Triclosan (2,4,4'-trichloro-2'-hydroxydiphenyl ether, Fig. 1) is a stable, lipophilic compound extensively used in hygiene products for more than 30 years. It provides immediate, persistent, broad-spectrum antimicrobial activity to properly formulated topical preparations. At low concentrations, triclosan appears bacteriostatic primarily by inhibiting one of the highly conserved enzymes (FabI) of bacterial fatty-acid biosynthesis. But it is bactericidal at higher concentrations, targeting at multiple cytoplasmic and membrane. However, the widespread and unregulated use of triclosan is highly controversial, with questions being raised about its effectiveness. As early as 1991, Cookson *et al.*[40] isolated MRSA strains that expressed low-level triclosan resistance from

patients who have been treated with daily triclosan baths for 2 weeks. Suller and Russel[41] isolated several *S. aureus* mutants with increased resistance to triclosan, which did not display increased resistance to antibiotics. Chuanchen *et al.*[42] have shown that triclosan is a substrate for three distinct efflux pumps (MexAB-OprM, MexCD-OprJ, and MexEF-OprN systems) in *P. aeruginosa*, indicating intrinsic resistance. Worse still, exposure of a susceptible strain to triclosan is more likely to promote the selection of multidrug-resistant (MDR) bacterial pathogens via overexpression of identical efflux systems and probably FabI target mutations, contributing to cross-resistance. Thus, it remains an open question in the use of triclosan to treat burn wounds.

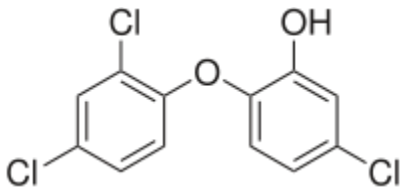

Fig. 1. Molecular structure of triclosan.

1.2.1.3 Quaternary ammonium (QA) salts.

QA salts have been known for many years as efficacious biocides against a broad range of microorganisms, being extensively used in clinic and industry. These compounds carry a positive charge at the N atom (Fig. 2) to attract negatively charged head groups of phospholipid in bacterial cell membrane, resulting in a variety of detrimental effects on microbes, including disruption of the cell structure, damage to cell membranes, interruption and denaturation of proteins and enzymes.[43-5] The antimicrobial activity of QA salt is closely linked to the length of N-alkyl chains. The most active compounds have linkers of 12-14 methylene units against Gram-positive bacteria and 14-16 against Gram-negative bacteria.[46-8]

Development of resistance toward QA salts among a diverse range of microorganisms, including pathogenic and non-pathogenic bacteria, has been well documented.[49-52] QA salts have low

chemical reactivity and will not be rapidly neutralized at the point of use, thus, it might expose bacterial cells to subinhibitory concentrations of QA salts in a long term and cause the emergency of resistant mutants with changes in their susceptibility. Bacterial resistance toward QA salts can be facilitated by several mechanisms, such as intrinsic membrane permeability barrier in Gram-negative bacteria, hyperexpression of efflux pump genes, acquisition of plasmid-encoded efflux pumps, modifications in the membrane composition, or expression of stress response and repair systems.[49] There is also increasing evidence of both coresistance and cross-resistance of QA salts and clinically relevant disinfectants and antibiotics, driving us to decrease the use of QA salts which contributes to the persistence and spread of multi-resistant genes.

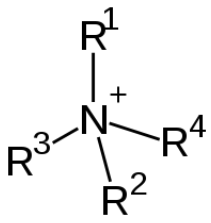

Fig. 2 Quaternary ammonium cation. The R groups can be the same or different alkyl or aryl groups. Also, the R groups can be connected.

1.2.1.4 Silver.

Silver products, such as silver-containing creams, have been widely used on burns to control the wound infection since the 1960s.[53] In recent years, a range of silver-coated or impregnated dressings have achieved great success in killing a broader range of bacteria than the cream base, including Actisorb Silver (Johnson & Johnson), Acticoat™ (Smith & Nephew), Urgotul SSD (Urgo), Aquacel Ag (ConvaTec), Contreet-H (Coloplast). Specifically, Acticoat™ remains as the most popular wound dressing in clinical settings. Acticoat™, consists of silver-based crystalline nanoparticles, exerted the most efficient and widest spectrum of antibacterial activity.[54] The non-

charged form of silver (Ag^0) reacts much more slowly with wound exudates (especially chlorine ions), thus being deactivated less rapidly in wounds. In vitro studies confirm that Acticoat™ provides a sustained release of silver for a minimum of 7 days, well suited for use in the management of burns and long-term wounds.[55-7] However, Acticoat™ is likely to adhere to a drying wound. It needs to be wetted before applying onto the wound and irrigated every 3 h to be kept moist.[58] Following pre-emptive analgesia before detachment, the dressing should be wetted again and gently peeled off.

Besides, the increase in the use of topical silver in the management of open wounds has raised another issue concerning silver resistance. Simon successfully defined the resistance to silver compounds which was encoded by genes located on plasmids or chromosome. Several bacterial strains including *E. coil* K-12, O157:H7, MRSA 133/03, 151 and 152 have been found to contain a silver-resistant gene: *silE*.[59-60] Although the clinical incidence of silver resistance remains low to date, it is becoming more important and urgent to screen out agents capable of inactivating pathogens without inducing resistance, in light of the likelihood of widespread bacterial resistance with the increasing usage of silver in many commercially available healthcare products.

1.2.1.5 *N*-chloramines.

A possible group of substitutes with low potential for developing resistance are *N*-chloramines, which have been extensively used for over 180 years due to their broad-spectrum antibacterial activity and long-term stability.[61-3] In *N*-chloramines, one or more chlorine atoms are covalently bonded to the nitrogen atoms by chlorination of imide, amide, or amine groups, thereby providing steady release of free active chlorine into the environment. The trend of their stability is determined by their structures, following the order below: imide < amide < amine *N*-chloramine, while the antimicrobial activity has an inverse trend of imide > amide >> amine *N*-chloramine.[64-5] *N*-

chloramines function as biocides via three steps: the first attack concerns the chlorination of external protein matrix of the bacterial (superficial chlorination), forming a moderate chlorine cover which does not impair the viability of bacteria; Meanwhile, *N*-chloramines can penetrate into intact membranes, diffuse throughout the cells, and initiate irreversible destruction of vitally important constituents, mainly S-H functions; After entering cells, oxidative reactions of active chlorine occur by targeting at thiol groups (cysteine) or thioethers (methionine), which constitute many critical enzymes and structures essential for cell survival. It leads to the inactivation and destruction of the microorganisms.[66] Until now, no bacterial resistance has been reported against *N*-chloramines since they have nonspecific interactions with protein sites. On the other hand, *N*-chloramine compounds, such as *N*-chlorotaurin, already exist in the human immune system, suggesting a broad tolerance. These two properties make *N*-chloramines the most attractive class of antiseptics.

Recently, Lingdong *et al.*[67] have developed new biocides combining with both *N*-chloramide and QA moieties, exhibiting distinctly enhanced bactericidal efficacy in solutions and after immobilized on surfaces as compared to *N*-chloramide alone. The mechanism of bacterial killing was proposed to hinge on the fact that the cationic QA center could attract the negatively charged cells and hence facilitated the transfer of active chlorine from *N*-chloramide to the cell's biological receptors upon direct contact. Unexpectedly, there was a decrease, not increase in the antibacterial efficiency of the "composite" biocides with the increasing alkyl chain length of QA moiety after being immobilized on poly(ethylene terephthalate) PET and cotton fabrics. It was attributed to the hydrophobic long alkyl chain showing a higher resistance to liquid flow of bacterial suspension in the surface layer, leading to less intimate contact between bacteria and the surface immobilized biocide. Even so, possible synergistic effect between *N*-chloramide and long-chained QA moiety

might exist in solutions considering their different antibacterial modes. This work is of great importance to develop novel, powerful antiseptics to overcome the raising issue of bacterial resistance.

1.2.2 Dressing adherence.

As previously mentioned, Acticoat^{TM}, the currently most widely used wound dressing, has a high tendency to adhere to the wound bed, causing discomfort and pain to patients. A significant burn is one of the most painful injuries a person can suffer, and dressing-related pain can sometimes be worse than pain from the burn wound. Common causes of wound pain and trauma include the removal of dressings stuck to the wound bed, stripping of peri-wound skin, and tissue maceration and excoriation due to poor management of wound exudate.[68-71] Byers[72] reported that burn patients suffered painful procedures in burn care, especially at dressing changes, tended to show higher degree of anxiety and lower pain threshold and tolerance. If left untreated, the pain and anticipatory anxiety may prolong and intensify into extreme fear and depression, even suicidal ideation.[73-5] Pain-induced stress can potentially delay wound healing and adversely affect patients' quality of life.

The glue-like nature of proteinaceous exudate is the main cause of adherence of dressings to wounds, forming the mechanical key upon drying. A secondary mechanism of adherence is also recognised that new tissue grows into the structure of the dressing and thus incorporates some of the dressing components into the healing wound.[76-7] Traditional dressings such as cotton gauze and simple dressing pads have a high tendency to adhere to any type of drying wound. They are easy to dry out by providing little occlusion and allowing evaporation of moisture. During this drying process, exudates soaked into the dressing fibres get hardening and non-viable tissue would adhere to the dressing, causing significant pain and tissue trauma on its removal. Thus, this type of

dressings should be changed frequently to avoid the dehydration, which is less cost effective. To address this situation, a myriad of non-adherent dressings have been developed to minimise dressing adherence and tissue disturbance, including alginates, hydrocolloids, and hydrogels. A non-adherent dressing can maintain a moist gel layer over the wound bed and is not expected to adhere provided that it is not allowed to dry out.

1.2.2.1 Modern dressings

1.2.2.1.1 Alginate dressings.

A large quantity of alginate dressings are used annually to treat moderate to heavily exuding wounds due to their powerful absorbency. Alginate dressings are formed form calcium alginate, which is a polymeric acid rich in α-L-guluronic acid (high-G) or in β-D-mannuronic acid (high-M). Once in contact with an exuding wound, the alginate dressing turns into a gel-like mass with a significant proportion of calcium ions in alginate exchanged with sodium ions in wound exudate. It helps maintain a physiologically moist microenvironment to promote wound healing and epidermal regeneration.[78-9] The first alginate dressing was Kaltostat (ConvaTec, Ickenham), a fibrous high-G calcium alginate. High-G fibers are capable of forming firmer structures with calcium ions and hence stronger gels than high-M fibers. But high-G alginate has a worse absorbency and gelling ability since the calcium ions are bound strongly and difficult to be replaced by sodium ions. Therefore, Kaltostat has been further modified to a mixture of calcium/sodium alginate in the ratio of 80/20, where the sodium ions are introduced into the fibers to improve the absorbency of the fibers. Sorbsan (Unomedical, Redditch) and Tegagel (3M, Loughborough) dressings are made of high-M calcium alginate fibers. Sorbsan dressing is made of an unneedled pressure rolled structure, while Tegagel is made of a hydroentangled structure

where the fibers are closely compressed. Typically, Sorbsan shows a lower degree of wet integrity than Tegagel due to its nonwoven structure.

However, a cytotoxic effect of calcium alginate dressings on fibroblasts and epidermal cells by direct contact or via the extraction medium *in vitro* was reported by Rosdy and Clauss.[80] It might be attributed to the high concentration of calcium ions released from the dressing, proved to inhibit the growth of cells in culture. Another problem of alginate dressings is foreign-body reactions (inflammation) induced by residual fibers in the wound site, which can potentially provoke complications such as the formation of hypertrophic scar and keloid.[81-2] Since alginate dressings require moisture to function effectively, they are contraindicated for use on dry wounds (full-thickness burns) or those with dry, hard, necrotic tissues.[32]

1.2.2.1.2 Hydrocolloid dressings.

Hydrocolloids are adhesive, wafer dressings that interact with exudate to form a moist gel at the wound surface. The first hydrocolloid dressing, Granuflex (ConvaTec, Ickenham), was introduced in the middle-1970s.[83] It has a complex structure, consisting of an inner layer of gel-forming agents (a mixture of sodium carboxymethylcellulose (CMC), gelatin and pectin) in an adhesive compound laminated onto a flexible, water-resistant outer layer. The outer layer acts as a thermal insulator and a barrier to micro-organisms in either direction. Until now, many manufacturers have produced a range of hydrocolloid dressings varying in chemical composition from the original formula. Two thin hydrocolloids Tegasorb (3M, Loughborough) and Duoderm Extra Thin (ConvaTec, Ickenham) are more favorable in the management of moist dermal wounds, as compared to Granuflex. Some formulations contain an alginate to increase absorption capabilities, such as Comfeel Plus™ (Coloplast, Peterborough) which is a hydrocolloid/alginate combination dressing. These hydrocolloid dressings allow the wound to remain moist due to the absorptive capacity of

hydrocolloid materials, facilitating the rehydration and debridement of dry, sloughy and necrotic wounds. But they are not recommended for clinically infected wounds such as diabetic foot ulcers or ischemic ulcers that require oxygen to heal rapidly due to the occlusive outer cover.[83-5] Worse still, they might encourage the growth of anaerobic bacteria. The outer layers of hydrocolloid dressings are typically impermeable to moisture vapor with a moisture vapor transmission rate (MVTR) of less than 300 g/m^2/24 hr, thus, these dressings should not be used on wounds with heavy exudate, which might cause maceration on the peri-wound skin and wound odor.[19] Moreover, the adhesive boarder of hydrocolloid dressings may strip fragile surrounding skin upon removal.

The hydrofiber Aquacel (ConvaTec, Ickenham) is a development of hydrocolloids by retaining their benefits but addressing the weakness such as aggressive adhesion. It is a soft, sterile, non-woven pad or ribbon dressing composed entirely of 100% sodium CMC. The dressing fibres of Aquacel swell and convert to a soft gel when in contact with wound fluid, retaining exudate and locking away harmful components within wound exudate, such as bacteria and proteinases. Walker and his coworkers[86] reported that Aquacel hydrofiber dressing had a superior ability to form a uniform, coadhesive gel structure which was highly effective in encapsulating large populations of pathogenic bacteria such as *P. aeruginosa* and *S. aureus*. Hydrofiber absorbs exudates directly into the fibres by vertical wicking, characterized with a rapid uptake of liquid. The absorbed wound exudate can be distributed to the entire dressing rather than just over the wound surface, creating a large fluid absorption capacity and thus giving longer wear time and fewer dressing changes. Hydrofiber dressings are most applicable to moderate to heavy drainage wounds (partial thickness burns), however, they appear to be easy to break apart after gelling and fibre residues may adhere to the wound bed upon drying.

1.2.2.1.3 Hydrogel dressings.

For many years hydrogel dressings, containing 80% or more water in a gel base, have been the main treatment option in burn care. Hydrogels are able to absorb exudate from moderate to lightly exuding wounds, and even donate moisture to a dry wound surface while allowing the passage of water vapour and oxygen. Hydrogel dressings are available either in amorphous form (a loose gel) or in a sheet form. Amorphous gels lessen in viscosity and become more fluid as they absorb exudate. They can be packaged in tubes, foil packets, or as saturated gauze pads. Amorphous hydrogels include products such as Aquaform® hydrogel and IntraSite Gel (Smith & Nephew, Hull), which are of the most benefit in the treatment of sloughy or necrotic wounds.[87] Amorphous gels can be used as wound fillers to fill in the "dead space", but a secondary dressing such as gauze is required to hold the hydrogel onto the wound bed which needs to be changed frequently. They can also be used when infection is present.

In contrast, sheet hydrogels, supported by a thin fiber mesh, do not need a secondary dressing. They can retain the shape as exudate is absorbed and can be cut to fit around the wound with or without adhesive borders due to the flexible nature. Various sheet hydrogels are available in the market including Hydrosorb (Hartmann, Heywood), ActiForm Cool (Activa Healthcare, Burton-on-Trent), Curagel (Tyco Healthcare, Gosport), Geliperm (Geistlich Pharma, Chester). Now evidence is accumulating that sheet hydrogels are very useful in pain management, particularly in superficial burns, as the moisture bathes nerve endings and the smoothing and cooling nature of hydrogels helps to reduce wound pain.[88-91] However, they are not recommended for wounds with heavy exudate due to the low absorption rate, which might cause periwound maceration and bacterial proliferation. Some sheet dressings are difficult to handle because of the low mechanical strength, thereby affecting patient compliance.

Hydrogels possess most of the desirable characteristics of an "ideal" dressing: they are non-adherent and cool the surface of the wound, significantly reducing dressing-change pain and discomfort; they provide a moist environment and even donate moisture to a dry wound to promote the healing without inducing any tissue reaction; they are also malleable and leave no residue due to the three-dimensional structure supported by cross-linked hydrophilic polymers; moreover, they are permeable to metabolites, possessing the huge potential of incorporating antimicrobials, growth factors and supplements. Hydrogels can be made by irradiation, freeze-thawing or chemical methods, but irradiation is considered as the most suitable tool for the formation of hydrogels.[92] The irradiating process is easy to control and the initiators or cross-linkers can be avoided which are harmful to human body. It is also possible to achieve the formation and sterilization of hydrogels in one step.

1.2.2.1.4 Atraumatic dressings.

"Atraumatic dressings", different with non-adherent dressings, are developed to overcome not only the problem of adherence to the wound bed but also the issue of damage to the surrounding skin. They rely on an adhesive technology (Safetac®) involving the use of "soft" silicone, a material that adheres gently to the peri-wound but do not adhere to moist wounds, thereby avoiding second trauma and reducing dressing-related pain.[76-7] The formation of a seal between intact skin and a dressing with Safetac® can prevent maceration by inhibiting the movement of wound exudates onto the surrounding skin. The first atraumatic dressing, Mepitel®, is a thin, porous wound contact layer consisting of a flexible polyamide net coated with soft silicone.[93] It should be used in combination with an outer absorbent dressing as multiple pores within Mepitel® allow the passage of wound exudate into the secondary absorbent layer. The nature of the bond formed between Mepitel® and the skin surface allows the dressing to be removed easily without damaging delicate new tissue

around the wound margin. Fowler[94] demonstrated that Mepitel® was frequently used on severe burns. Mepilex® Border and Mepilex® Transfer are advanced products in this range, with a perforated Safetac® layer underneath an absorbent core which effectively absorbs and retains exudate and maintains a moist environment.

Mepilex® Ag is antimicrobial, absorbent, soft silicone foam dressing that is designed for patients with exuding wounds, such as burns which are exposed to high risk of infection.[95] Walker and his coworkers[96] have conducted the antimicrobial test of Mepilex® Ag against *P. aeruginosa* and *S. aureus* using a seeded-agar microbial model, where the silver-containing dressing was applied onto an agar plate seeded with 1×10^5 CFU/mL of bacteria. After 48-hour dressing contact period and a further 24-hour incubation of the plate with the dressing removed, growth of both microbes was observed in the seeded-agar beneath the Mepilex® Ag foam dressing. The contact layer of soft silicone of Mepilex® acts as a physical barrier to the availability of silver, thereby failing to prevent bacterial proliferation. It also tends to produce a higher cell adherence, particularly in the presence of hydration. In comparison, hydrogel dressings incorporated with silver exhibited excellent antibacterial activity with negligible growth of bacteria. Overall, hydrogels demonstrate the huge potential as burn wound dressings for providing numerous advantages as mentioned above.

1.2.2.2 Evaluation of dressing adherence.

In order to study the adhesion of wound dressings, it is highly desirable to have a model for quantitative evaluation of skin damage at dressing removal. Mutsumura[97] introduced a simple, rapid *in vitro* method of applying wound dressings onto plain copy paper printed with black ink. The amount of black toner stripped from each paper was examined using a high-power videoscope at the removal of dressing, correlated with the quantification of the epithelium and stratum corneum *in vivo*. Similarly, Waring[98] applied a stain to the health human skin and measured the

intensity of the stain after repeated application and removal of dressings. However, the printed paper or the health human skin is considered as purely static, which cannot appropriately reflect the real situation of dynamic wound healing. The wound healing process is very complex, consisting of four phases of inflammation, granulation tissue formation, matrix remodeling and re-epithelialisation.[99] Extracellular matrix proteins (exudates) at the dressing-wound interface become "viscous glue" upon drying, causing dressing adherence to the wound bed. Besides, cells involved in wound healing, such as fibroblasts present in granulation tissue and keratinocytes responsible for re-epithelialisation, come into direct contact with primary dressings and keep proliferating and migrating onto dressings.

Cochrane[100] developed a bioadhesion model with a pre-soaked wound dressing placed on to the surface of the cell culture dish with the application of minimum force to maintain the cell-dressing contact. After the defined period of time, the dressing was carefully removed with minimum force to avoid any cell damage or cell detachment. The number of cells attached to the dressing was assessed with qualitative and quantitative techniques. The mechanism of this bio-adhesion model was supposed to be that proteins adsorbed onto the pre-soaked dressings act as "glue", resulting in cellular attachment to the dressings. But the application of external force in this method is a big variation, which might significantly influence the cell adhesion. Instead of applying the dressing to the cell surface, Rogers[101] added the cell suspension onto the dressing surface for seeding, which was prevalent in researchers to evaluate cell adhesion to dressings. In these tests, the cell-dressing complex is not allowed to dry, thereby failing to mimic clinical conditions of the dressing "drying out" on the wounds. The process of wound desiccation plays a very important role in dressing adherence, which is the biggest limitation of this model.

Dong[102] developed a device for measuring adherence of skin grafts to full-thickness wounds on mice. 2×2 cm^2 of grafts were applied to the wound on mice, which was clamped and placed on a platform. The graft was peeled off with a device of motor at a constant rate rotation of 2 RPM and the peeling force was recorded by the installed force transducer. This *in vivo* model provided a reproducible, controlled, constant rate peeling process, accurately measuring the force required to overcome the adhesion of the graft to the wound surface at each healing phase. It is useful for the study of adherence properties of wound dressings. However, using animals in research for screening purposed is of ethical concerns, moreover, it requires a huge expenditure. These animals kept in unnatural conditions are quite different from humans, so the consequences of animal testing may not be applicable to humans. *In vivo* evaluation of wound dressing performance on human beings is more direct but not without drawbacks. It is difficult to obtain a reproducible and valid measurement in clinical settings as either wound type or psychological aspect varies a lot with each patient.

Andrews and Kamyab[103] established a wet-gelatin model to study the adhesion of dressings. Gelatin is a strongly hydrogen-bonded, proteinaceous material which has a capacity for adhesion, similar to wound exudates. The gelatin solution was brought into contact with the dressing and allowed to dry progressively through the gel state into a rigid solid, perfectly imitating the process of wound desiccation. Different clinical situations could be simulated by allowing the gelatin to dry to different extents. After the chosen drying period, the dressing material was peeled from the solidified gelatin at a $180\,°$ peeling angle, with an Instron testing machine to obtain the results of peeling force, and the average peeling force was then converted to a peeling energy. This *in vitro* model is very convenient, time-saving and informative. It was found that the peeling energy increased with the drying time due to the loss of water in gelatin, which vacated available hydrogen

bonding sites to the dressing surface. The more water content of the gelatin, the lower adherence to wound dressings. It behaves in a similar manner to a drying wound exudate. The peeling energy is also temperature dependent, but *in vivo* applications are more related to the surface temperature of the human skin (32 ℃).

1.3 Controlled drug release.

Controlled release dressings serve as a biocompatible support, which contains the antimicrobials to be consistently and sustainedly delivered to wound sites, thereby avoiding frequent dressing change. It is particularly useful and efficient in infection control during the tissue repair process of burns. Most modern dressings are made from polymers, which are capable of incorporating with therapeutic agents and delivering them to wound sites as vehicles. Specifically, hydrophilic polymers have been extensively used as controlled release dressings, such as hydrogels, hydrocolloids and alginate dressings.[104-5] Some polymeric dressings are prepared in novel formulations using polymeric biomaterials such as collagen, chitosan and hyaluronic acid,.[106-8] Swellable dressings for controlled drug delivery comprise synthetic polymers, including silicone gel sheets, lactic acid, and so on.[109-10] There are also some reports about composite dressings constituting both natural and synthetic polymers.[111-2]

Drug-polymer systems can be broadly categorized into three main processes: diffusion-controlled system, swelling-controlled system, and erosion-controlled system.[113-4] Specifically, diffusion-polymer systems can be further classified into reservoir systems where the drug is retained in a central compartment and surrounded by a polymeric membrane through which it must diffuse, and matrix systems where the drug is homogeneously dispersed within the polymer matrix. Swelling-controlled systems further enhance the drug diffusion due to polymer swelling and hydrogels are probably the most common vehicles in this system. Upon contact with a moist wound surface,

hydrogels are able to absorb wound exudate and swell into a gel over the wound bed. The swollen, cross-linked network has an acutely increased water content and polymer free volume, typically comprising 60-90% fluid and 10-40% polymer and thus enabling the diffusion of preloaded drugs to wound sites.[113] The drug release gradually slows down due to the decreased concentration gradient of drugs in the polymer and external environment. But in erosion-controlled systems, after diffusion and swelling, polymer degradation and erosion prevailingly controls the latter part of release profiles. These matrixes are based on soluble polymers, which can degrade and eventually disintegrate and dissolve in consequence of natural biological process. They are particularly popular in oral delivery systems and injected delivery systems, instead of transdermal delivery systems. In the context of this study, a swelling-controlled drug delivery system is more relevant for non-adherent hydrogel dressings.

Hydrogels are capable of swelling in aqueous medium. The first water molecules, also called bound water, enter the polymeric matrix and interact with the polar and hydrophobic groups of hydrogels successively, resulting in the expansion of the gel network. After that, additional water, which is named free or bulk water, will be imbibed to fill the space between the network chains towards infinite dilution. The continuous stretching of the network will be counter-balanced by the cross-linked system. The disintegration and dissolution of gel starts if the network chains or crosslinks are degradable. In general, the water permeation and diffusion into hydrogels, in conjunction with the degradation of hydrogels can be controlled by the polymer composition.[115-7] The composition can be manipulated to accommodate multifarious drugs loaded into the matrix depending on the physical properties of drugs, loading level, and desired release kinetics. Typically, there are two methods for loading drugs into hydrogels: (1) in-situ loading where the hydrogel precursor solution is mixed with a drug, an initiator, and a cross-linker, and allowed to polymerize,

encapsulating drugs within the synthesized matrix simultaneously; (2) post-loading where a preformed hydrogel is allowed to swell to equilibrium in a suitable drug solution and then the drug is absorbed to this matrix.[115, 118] The drug-loaded hydrogel is then dried for later use. The first approach is inapplicable when the polymerization conditions have deleterious effects on drug properties. Besides, it is quite difficult to purify the drug-polymer system when loading and polymerization are carried out in one step. Thus, drug loading by the swelling method is more favorable due to the potential advantages it offers. The subsequent drug release from hydrogels involves the hydration of the polymer by fluids and simultaneous desorption of drugs via diffusion, which can be modeled with the swelling-controlled system as described above.

1.4 Conclusions.

Burns injuries are a major cause for hospitalization, associated with significant morbidity and mortality. Most deaths of burn patients today result from infections rather than burns themselves, about 75% of the mortality following burn injuries being related to infections.[21] A new generation of wound dressings incorporated with pharmaceutical agents is widely used in clinical to prevent or combat burn infections. Specifically, the incorporated agents play a dominant role including antibiotics and various antiseptics. Silver is the most popular remedy used by burn care providers because of the broad-spectrum antibacterial activity. Although there are few adverse effects reported in clinical uses, silver-resistant genes have been isolated in several bacterial strains in lab. To address this situation, it is urgent to develop agents capable of inactivating pathogens without inducing bacterial resistance. Organic *N*-chloramines have been in clinical use for over 180 years thanks to their effectiveness toward a broad spectrum of microorganisms, and no resistance has been yet reported.[66] *N*-chloramines are less likely to induce resistance because they attack multiple peptide and protein targets in bacteria. Furthermore, it was found the bactericidal efficacy of *N*-

chloramine could be boosted after tethering with a cationic quaternary ammonium (QA) center. The novel "composite" compound might have great potential to be used as a topical antiseptic. One way of its use is to incorporate in wound dressings.

Another concern of current wound dressings is the high tendency to adhere to a drying wound bed, causing significant pain and tissue trauma. A categorise of "non-adherent" as well as "atraumatic" dressings has been developed to alleviate this problem. Hydrogels are considered as the most desirable non-adherent dressings for providing a moist gel layer over the wound bed to avert dressing-removal pain and trauma and promote the wound healing. More important, the cross-linked macromolecular network of hydrogel can serve as a reservoir to deliver drugs to wound sites, achieving a both non-adherent and antibacterial wound dressing. An *in vitro* gelatin model for dressing adherence evaluation overcomes the disadvantages associated with traditionally cell adhesion test or *in vivo* test which can be expensive, time-consuming, and sometimes ethically questionable as a screening tool.[103]

CHAPTER 2. HYPOTHESES AND OBJECTIVES

This project aims to solve three problems: 1. Establishment of a cheap and versatile *in vitro* model to evaluate the adherence of wound dressings to wounds; 2. Improvement of the adherence profile of burn dressings; 3. Exploration of an alternative antibacterial agent to silver in view of the emerging resistance associated with silver based wound dressings. It is hypothesized that 1. The wet-gelatin model can be further improved to better simulate the clinical situation under certain conditions such as drying at relatively high humidity; besides, water and surfactant solution treatment prior to detachment can help ease the peeling of dressings from the gelatine model; 2. If a thin layer of hydrogel is grown from fibers of the base dressing fabric, non-adherent property can be imparted without compromising dressing flexibility; 3. Covalently combining *N*-chloramide and QA moieties in the same structure might result in more potent broad-spectrum bioactive agents, which are less likely to induce bacterial resistance; 4. The diffuse rate of biocides can be controlled by the network structure of the deposited hydrogel to achieve minimal cytotoxicity and satisfying antibacterial efficacy. Specifically, I will:

1. Establish an *in vitro* dressing peeling model to better approximates the clinical environment and also provide a short-term solution for decreasing the adherent property of wound dressings currently used in hospitals and burn care centers.
2. Graft a thin layer of hydrogel onto the surface of poly(ethylene terephthalate) (PET) fabric via UV irradiation to achieve a highly flexible and non-adherent surface. PET fabrics are among the most representative base materials in burn wound dressings (Acticoat™ and Atrauman®) in view of their readily availability, good biocompatibility and excellent mechanical strength.
3. Synthesize a series of new compounds combining both *N*-chloramide and QA moieties (Scheme 1) to study the possible synergistic bactericidal effect of these two components in solution.

4. Load these new biocides into the hydrogel network and control the release of biocides to achieve a consistent, effective infection control in burn wounds.

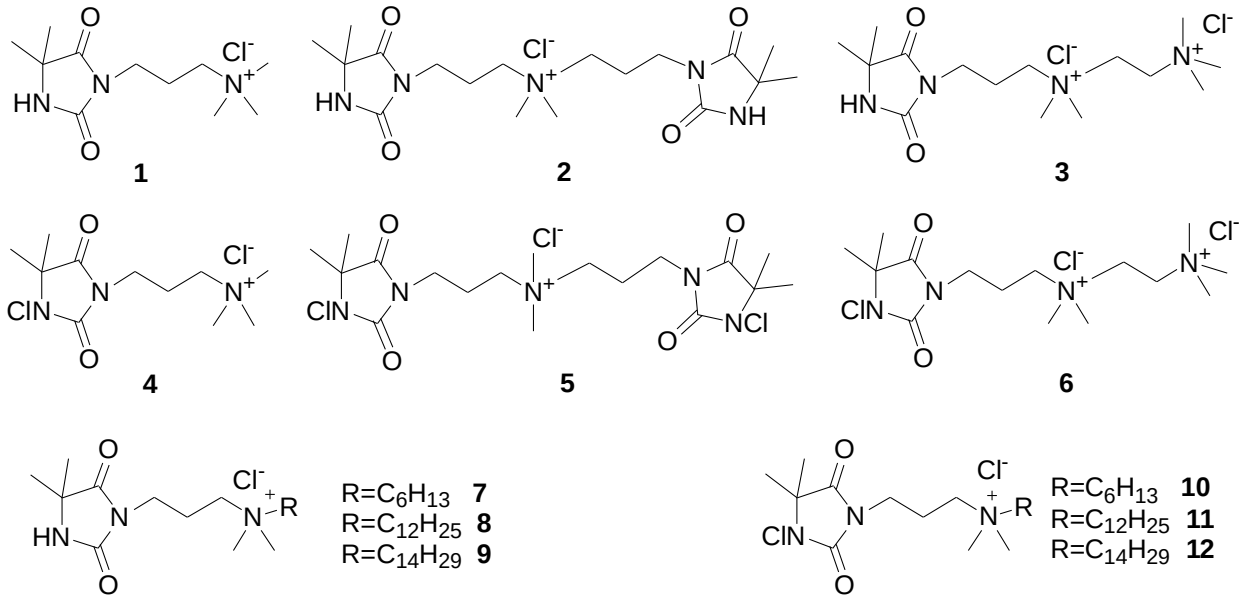

Scheme 1. Structures of N-Chloramine precursors (**1-3**, **7-9**) and end products (**4-6**, **10-12**).

CHAPTER 3. MATERIALS AND METHODS

3.1 Materials.

Acrylamide (AM) and N,N'-methylene bisacrylamide (MBA, crosslinker) were purchased from Sigma-Aldrich (Oakville, ON). Gelatin was purchased from Fisher Scientific (Ottawa, ON). PET plain woven fabric (#777H) was purchased from Testfabrics, Inc. (West Pittiston, PA).

Reagents and solvents used in chemical synthesis, bacteria and mammalian cell assays were obtained from commercial suppliers such as Sigma, VWR or Fisher. All chemicals were analytical grade and used as received without further purification unless otherwise stated. Synthetic compounds were purified using flash column chromatography on silica gel obtained from Selecto Scientific Georgia USA. NMR spectra were recorded at room temperature in 5 mm NMR tubes on a Bruker Avance 300 MHz NMR spectrometer. Accurate mass measurements were performed using a PerkinElmex Sciex prOTOFTM 2000 MALDI-OTOF Mass Spectrometer. Community-associated (CA)-MRSA and multi-drug resistant (MDR) *P. aeruginosa* were used as the model microorganism to challenge all the biocides. Both were clinical strains obtained from the University of Alberta Hospital, with the genotypes of CA-MRSA 40065 and MDR *P. aeruginosa* 73104. ACTT-PCS-201 neonatal human dermal fibroblasts were purchased from ATCC (Canada).

3.2 Experiments.

3.2.1 Adaption of the wet-gelatin model for adherence evaluation.

An *in vitro* wet-gelatin model was chosen to mimic the environment between human skin and wound dressing.[103] Briefly, a polytetrafluoroethylene (PTFE) window frame with an open area 16×60 mm^2 for gelatin casting wad created. All the fabric samples (3 × 13 cm^2) were soaked in deionized (DI) water for 5 min, centrifuged for 30 s and then spread on a clean bench; one frame

was placed onto each piece of fabric. 40% w/w gelatin solution was prepared in 70 ℃ DI water and then poured into the window frame. To simulate the wound desiccation process, the whole module with gelatin on the top of dressing was dried in the incubator at the skin temperature 32 ℃ for different time durations, while maintaining a dry (< 25% RH) or humid (75% RH) environment. Sulfuric acid (H_2SO_4) was used to maintain a constant humidity as per previously published protocols.[134] After a period of time (4, 8, 16, 24 h), the PTFE window was removed from the specimen and an Instron 5956 machine (Instron, MA, USA) was used to peel the gelatin off the sample at a constant rate of 100 mm/min with 180 ° peeling angle. The five highest peaks were chosen to obtain the average force. Peeling energy per unit area (J/m^2) was expressed in this thesis as: $\theta = \frac{2P}{b}$, where P was the average peeling force and b was the width of the gelatin strip (1.6 cm).

3.2.2 Preparation of hydrogel deposited PET.

PET plain woven fabric (6 × 14 cm) was first extracted with deionized (DI) *water* for 24 h to remove impurities before any treatment. The extracted PET fabric was treated with O_2 plasma (flow rate of O_2: 2-4 standard cubic centimeter per minute) for 20 min to produce peroxide functional groups on the surface of the fabric. 3 mL monomer solution containing 9.8% (w/v) AM and 0.2% (w/v) MBA was uniformly placed onto the plasma treated PET fabric. Then the fabric was sandwiched by two glass plates prior to UV irradiation (365 nm, 3000 $\mu w/cm^2$). Crosslinked polyacrylamide (PAm) hydrogel was grown from the surface of PET after UV irradiation as shown in Scheme 2.

After the radical grafting crosslinking copolymerization, the PET sample was extracted with DI water in a 65 ℃ water bath at the shaking speed of 150 RPM for 16-24 hours to remove ungrafted monomers and polymers, dried and stored in a desiccator to reach constant weight. The resultant

PET fabric is referred to as "PET-PAm". The amount of hydrogel deposited was calculated by the weight increment of the PET fabrics after the polymerization as follows.

$$\text{Weight increment} = (W_t - W_0)/W_0 \times 100\%$$

where W_0 is the weight of untreated PET and W_t is the weight of sample after t min of UV irradiation, t = 30, 50 and 70 min.

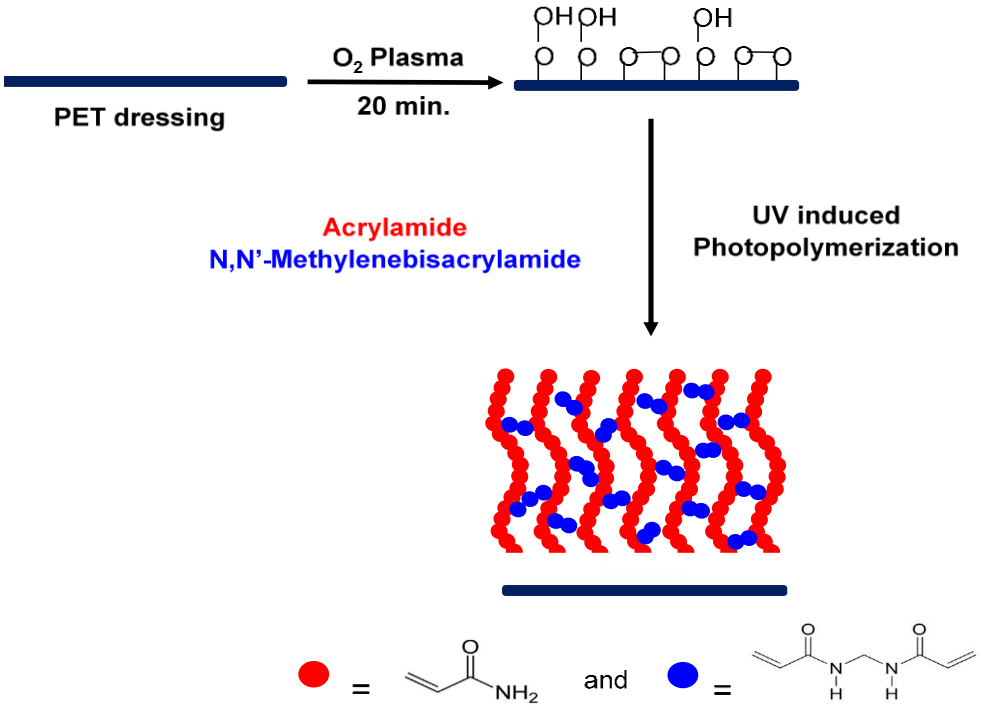

Scheme 2. Surface grafting with polyacrylamide (PAm) hydrogel onto PET dressing via plasma treatment and photopolymerization.

3.2.2.1 Flexibility test.

A Cantilever Bending Tester was used to test the flexibility of fabric samples according to ASTM standard D 1388-96.[119] Briefly, a fabric sample was immersed in DI water for 5 min and centrifuged for 30 s at 2800 rpm to remove the excess water adsorbed on the surface. Then the swollen sample (2 × 12 cm^2) was put on a horizontal platform and slid gradually in a direction parallel to its long dimension. The length overhang was measured at which the tip of the specimen

was depressed under its own mass to the point where the line joining the top to the edge of the platform made a 41.5 ° angle with the horizontal. Samples were tested at both ends and the two readings were averaged. The bending length c and flexural rigidity were then calculated:

c = o/2, where c = bending length (cm), o = length of overhang (cm);

$G = W \times c^3$, where G = flexural rigidity (mg•cm), W = fabric mass per unit area (mg/cm^2).

3.2.2.2 Swelling ratio test.

Before the peeling force test, fabric samples were immersed in DI water for 5 min and centrifuged for 30 s at 2800 rpm to remove the excess water adsorbed on the surface. The swelling process was confirmed by change in weight: the ability for swelling is called "swelling ratio".

$$\text{Swelling ratio} = (M_1-M_0)/M_0 \times 100\%$$

where M_0 is recorded as the weight of dry sample, and M_1 is the weight of swollen sample.

3.2.2.3 Adherence evaluation.

The wet-gelatin model was used to test the evaluation of the prepared PET-PAm dressings to study the effect of hydrogel on decreasing the adherence of wound dressing. The procedure was the same with that in the section 3.2.1.

3.2.3 Synthesis of new "composite" biocides.

The chemical synthesis of new biocides is depicted in Scheme 3, except for compound **1** and **4** which were prepared according to previously published protocols.[67]

Synthesis of compound 2: To the solution of bromide **13** (1.2 g, 4.8 mmol) in EtOH solution (30 ml EtOH + 3 ml H_2O) was added dimethylamine hydrogen chloride (1.96 g, 24 mmol) and NaOH (0.96 g, 24 mmol). The resulting solution was heated to reflux overnight. After the solvent was

removed, the residue was purified by column chromatography eluting with MeOH/CH_2Cl_2 (1:5, v/v) to give **15** as white solid (0.7g, 51%).

^{1}H NMR (D_2O, 300 MHz, δ) 3.55 (t, *J* =7.5 Hz, 2H), 2.65 (t, *J* =7.5 Hz, 2H), 2.46 (s, 6H; $N(CH_3)_2$), 1.88 (m, 2H;), 1.44 (s, 6H); ^{13}C NMR (D_2O, 75 MHz, δ) 181.0, 157.3, 58.8, 55.6, 43.6, 36.0, 24.3, 23.7; HRMS (MALDI-TOF) m/z: $[M+H]^+$ calculated for $C_{10}H_{20}N_3O_2^+$, 213.1550; found: 213.1555.

To the solution of **15** (0.25 g, 1.17 mmol) in 10 ml CH_3CN was added bromide **13** (0.32 g, 1.1 equiv). The reaction mixture was allowed to undergo reflux for 24 hours. Solvent was removed and the crude product was applied on chromatography column (MeOH/CH_2Cl_2, 1:3, v/v) to give Br^- form product, which was dissolved in a minimum amount of water and slowly passed through an anion-exchange resin (Amberlite R IRA-900, Cl^- form) to afford **2** as white solid (0.46 g, 94%)

^{1}H NMR (D_2O, 300 MHz, δ) 3.6 (t, *J* = 6 Hz, 2H), 3.37 (t, *J* = 7.5 Hz, 2H), 3.12 (s, 3H), 2.10, (m, 2H), 1.45 (s, 6H) ; ^{13}C NMR(D_2O, 75 MHz, δ) 180.7, 157.1, 61.3,59.2, 50.8, 35.2, 23.6, 21.2; HRMS (MALDI-TOF) m/z: $[M-Cl]^+$ calculated for $C_{18}H_{32}N_5O_4^+$, 382.2449; found: 382.2454.

Synthesis of Compound 3: To the solution of bromide **13** (1.5g, 6.02 mmol) in 25 ml CH_3CN was added N,N,N',N'-Tetramethylethylenediamine (4.5 mL, 5 equiv). The resulting solution was heated to gentle reflux for 18 hours. Then solvent and excess tert-amine was removed the residue was purified by column chromatography (MeOH/CH_2Cl_2, 1:3, v/v) to give **14** as yellowish oil (1.3g, 76%).

^{1}H NMR (D_2O, 300 MHz, δ) 3.61 (t, *J* = 6.0 Hz, 2 H), 3.49 (t, *J* = 7.5 Hz, 2 H), 3.41 (t, *J* = 6 Hz, 2H), 3.15 (s, 6 H), 2.83 (t, *J* = 7.5Hz, 2H), 2.30 (s, 6H), 2.09-2.18 (m, 2H), 1.45(s, 6H); ^{13}C NMR($CDCl_3$, 75 MHz, δ) 180.57, 157.04, 61.8, 60.7, 59.2, 53.5, 44.4, 43.7, 35.4, 23.6, 21.4; HRMS (MALDI-TOF) m/z: $[M-Br]^+$ calculated for $C_{14}H_{29}N_4O_2^+$, 285.2285; found: 285.2290.

To the solution of **14** (0.9 g, 3.15 mmol) in 30 mL mixed solvent CH_3CN/CH_3OH (2:1, v/v) was added excess methyl iodide (2 mL, 10 equiv). The resulting solution was continuously stirred at room temperature for 22 hours before solvent and excess of methyl iodide were removed under vacuum. The oily residue was purified by column chromatography ($MeOH/CH_2Cl_2$, 1:3-1:2, v/v) to give I^- form product as yellow solid. Then product was dissolved in minimum amount of water and slowly passed through an anion-exchange resin (Amberlite R IRA-900, Cl^-) to afford **3** as white solid (0.87 g, 74%).

^{1}H NMR (D_2O, 300 MHz, δ) 4.03 (s, 4H), 3.63 (t, *J* = 7.5Hz, 2H), 3.54(t, *J* = 7.5Hz, 2H), 3.32 (s, 15H), 2.21 (m, 2H), 1.46 (s, 6H); ^{13}C NMR($CDCl_3$, 75 MHz, δ) 180.7, 156.8, 63.1, 59.3, 56.3, 57.5, 53.8, 35.2, 23.4, 21.4.

Synthesis of Compound 7-9: To the solution of **15** (1.68 g, 7.89 mmol) in CH_3CN (40 mL) was added bromohexane, bromododecane or bromotetradecane (1.5 equiv.). The resulting solution was heated with stirring to gentle reflux for 24 hours. Then solvent was removed and the residue was purified by column chromatography ($MeOH/CH_2Cl_2$, 1:3) to afford the corresponding Br^- form product (**7**, 90%; **8**, 92% and **9**, 88%), which was dissolved in a minimum amount of water and slowly passed through an anion-exchange resin (Amberlite R IRA-900, Cl^-) to afford Cl^- form product as white solid.

7 ^{1}H NMR (D_2O, 300 MHz, δ) 3.62 (t, *J* = 6.6 Hz, 2 H), 3.28-3.37 (m, 4 H), 3.09 (s, 6 H), 2.09-2.17 (m, 2 H), 1.70-1.75 (m, 2H), 1.45 (s, 6 H), 1.35-1.40 (m, 6 H), 0.90 (t, *J* = 6.4 Hz, 3 H); ^{13}C NMR (D_2O, 75 MHz, δ) 180.6, 157.1, 64.1, 60.7, 59.2, 50.9, 35.4, 30.4, 25.0, 23.5, 21.8, 21.6, 21.2, 13.2; HRMS (MALDI-TOF) m/z: $[M-Cl]^+$ calculated for $C_{16}H_{32}N_3O_2^+$, 298.2489; found: 298.2494.

8 ^{1}H NMR (D_2O, 300 MHz, δ) 3.62 (t, *J* = 6.2 Hz, 2 H), 3.41-3.43 (m, 4 H), 3.18 (s, 6 H), 2.14-2.17 (m, 2 H), 1.76-1.77 (m, 2H), 1.47 (s, 6 H), 1.32-1.40 (m, 18 H), 0.92 (t, *J* = 6.3 Hz, 3 H); ^{13}C NMR (D_2O, 75 MHz, δ) 179.7, 156.8, 63.8, 60.7, 58.9, 51.3, 35.5, 31.9, 29.7, 29.6, 29.4, 29.0, 26.0, 23.9, 22.6, 22.3, 21.5, 18.9; HRMS (MALDI-TOF) m/z: $[M-Cl]^+$ calculated for $C_{22}H_{44}N_3O_2^+$, 382.3428; found: 382.3433.

9 ^{1}H-NMR ($CDCl_3$, 300 Hz) 3.60 (t, *J* = 6.7 Hz, 2H), 3.31-3.38 (m, 4 H), 3.15 (s, 6 H), 2.09-2.14 (m, 2H), 1.71-1.73 (m, 2H), 1.44 (s, 6 H), 1.31-1.37 (m, 22 H), 0.91 (t, *J* = 6.7 Hz, 3 H); ^{13}C-NMR ($CDCl_3$, 75 Hz) 179.6, 156.8, 63.5, 60.6, 58.9, 51.2, 35.4, 31.9, 29.9, 29.8, 29.7, 29.0, 26.0, 23.8, 22.6, 22.2, 21.4, 13.1; HRMS (MALDI-TOF) m/z: $[M-Cl]^+$ calculated for $C_{24}H_{48}N_3O_2^+$, 410.3741; found: 410.3746.

Chlorination of the *N*-chloramide precursors: To the solution of non-chlorinated compound (**2, 3, 7-9**) in mixed solvent (*t*-BuOH:H_2O，4:1，v/v), 3 equivalent excess *t*-butyl hypochlorite was added. The reaction was allowed to stir vigorously for 22-24 h (except **3**). Due to poor solubility in this mixed solvent, the chlorination of **3** was prolonged to three days to reach satisfactory conversion. Excess *t*-butyl hypochlorite and solvent were removed under vacuum and the corresponding chlorinated forms **(5**, **6**, **10-12**) were thus obtained as white solid.

5: ^{1}H NMR (D_2O, 300 MHz, δ) 3.7 (t, *J* = 7.5Hz, 2H), 3.37 (t, *J* = 4.5Hz, 2H), 3.13 (s, 3H), 2.13, (m, 2H), 1.53 (s, 6H); ^{13}C NMR (D_2O, 75 MHz, δ) 176.7, 155.4, 66.5 61.3, 50.9, 36.5, 21.3, 20.9; HRMS (MALDI-TOF) m/z: $[M-Cl]^+$ calculated for $C18H30Cl_2N_5O_4^+$, 450.1669; found: 450.1675.

6: ^{1}H NMR (D_2O, 300 MHz, δ) 4.03 (m, 4 H), 3.72 (t, *J* = 6.8 Hz 2 H), 3.56 (t, *J* = 7.4 Hz, 2 H), 3.32 (s, 9 H), 3.26 (s, 6 H), 2.21-2.26 (m, 2 H), 1.49 (s, 6H); ^{13}C NMR (D_2O, 75 MHz, δ) 176.9, 155.6, 63.3, 59.3, 57.9, 56.5, 53.5, 51.2, 35.3, 23.4, 21.2;

10: ^{1}H NMR (D_2O, 300 MHz, δ) 3.71 (t, *J* = 6.4 Hz, 2 H), 3.29-3.38 (m, 4 H), 3.09 (s, 6 H), 2.09-2.18 (m, 2 H), 1.71-1.76 (m, 2H), 1.53 (s, 6 H), 1.35-1.41 (m, 6 H), 0.91 (t, *J* = 6.5 Hz, 3 H); ^{13}C NMR (D_2O, 75 MHz, δ)176.8, 155.4, 66.3, 64.2, 60.6, 50.8, 36.6, 30.4, 29.6, 25.0, 21.7, 21.1, 21.0, 13.2; HRMS (MALDI-TOF) m/z: $[M\text{-}Cl]^+$ calculated for $C_{16}H_{31}ClN_3O_2^+$, 332.2099; found: 332.2105.

11: ^{1}H NMR (D_2O, 300 MHz, δ) 3.74 (t, *J* = 6.0 Hz, 2 H), 3.33-3.37 (m, 4 H), 3.16 (s, 6 H), 2.15-2.17 (m, 2 H), 1.76-1.77 (m, 2H), 1.52 (s, 6 H), 1.32-1.38 (m, 18 H), 0.92 (t, *J* = 6.0 Hz, 3 H); ^{13}C NMR (D_2O, 75 MHz, δ) 175.7, 155.0, 66.1, 60.7, 59.9, 51.7, 36.7, 31.9, 29.7, 29.6, 29.4, 29.3, 25.8, 22.6, 22.2, 21.5, 21.3, 13.9; HRMS (MALDI-TOF) m/z: $[M\text{-}Cl]^+$ calculated for $C_{22}H_{43}ClN_3O_2^+$, 416.3038; found: 416.3044.

12 ^{1}H-NMR ($CDCl_3$, 300 Hz) 3.73 (t, *J* = 6.7 Hz, 2H), 3.26-3.40 (m, 4 H), 3.16 (s, 6 H), 2.12-2.17 (m, 2H), 1.66-1.70 (m, 2H), 1.51 (s, 6 H), 1.31-1.37 (m, 22 H), 0.92 (t, *J* = 6.7 Hz, 3 H); ^{13}C-NMR ($CDCl_3$, 75 Hz) 175.5, 155.0, 66.0, 59.7, 59.7, 51.8, 36.7, 32.0, 29.9, 29.8, 29.6, 29.5, 29.0, 25.9, 22.7, 21.5, 13.9; HRMS (MALDI-TOF) m/z: $[M\text{-}Cl]^+$ calculated for $C_{24}H_{47}ClN_3O_2^+$, 444.3351; found: 444.3357.

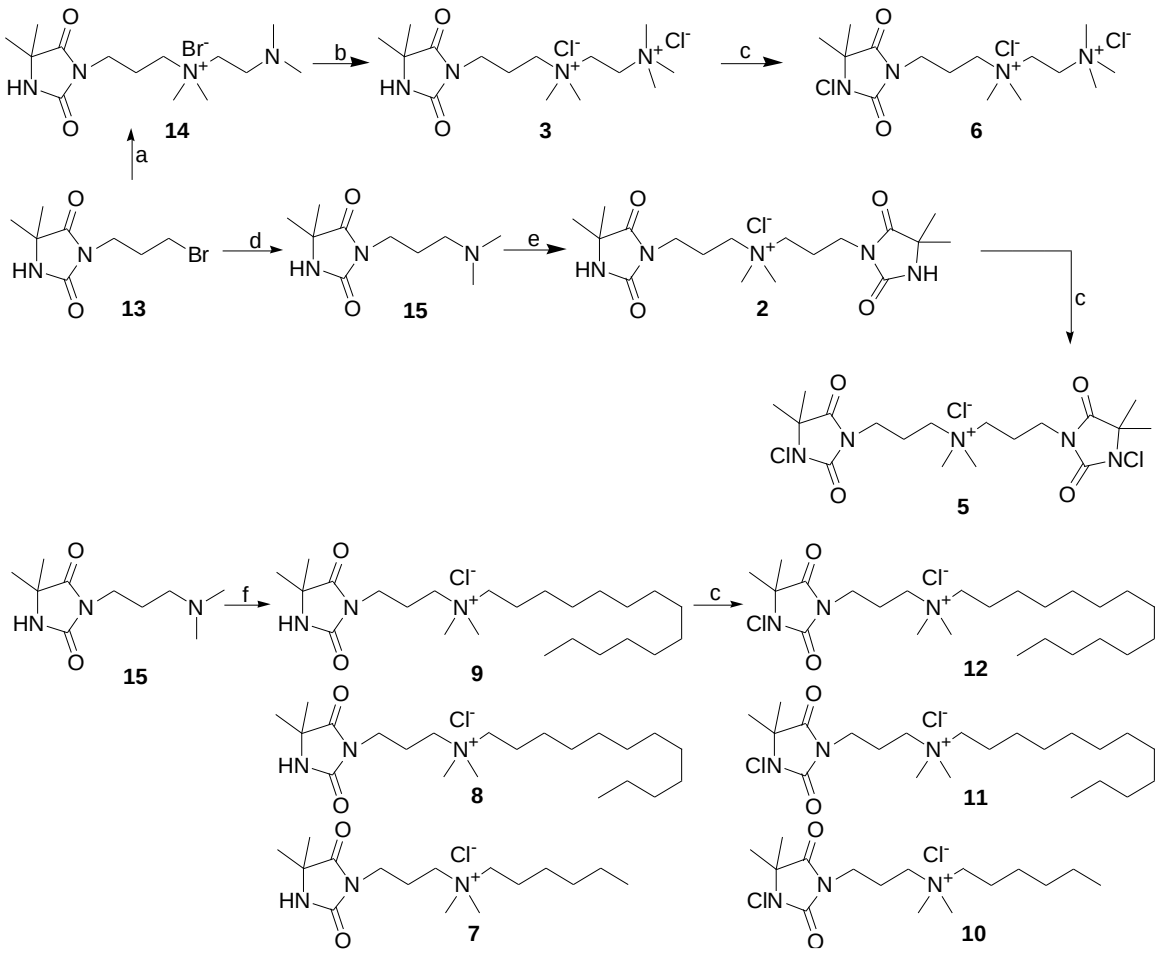

Scheme 3. Chemical synthesis of the end products except for compound **4**. Reagents and conditions: a) 5 equiv. N,N,N',N'-tetramethylethylenediamine, CH_3CN, reflux, 18 h, 76%; (b) 10 equiv. MeI, CH_3CN/CH_3OH (2:1) rt, 22 h, 74%, then Amberlite R IRA-900 resin (Cl^- form); (c) 3 equiv. *t*-butyl hypochlorite, *t*-BuOH:H_2O (4:1), rt, quantitative yield; d); (d) 5 equiv. dimethylamine hydrogen chloride, 5 equiv. NaOH, 90% EtOH, relux, overnight, 52%; (e) Bromide **22**, CH_3CN, reflux, 24 h, 94%; (f) 1.5 equiv. bromohexane, bromododecane or bromotetradecane, CH_3CN, reflux, 24 h.

3.2.3.1 Static antibacterial assessment of all the compounds.[120]

For the static antibacterial studies, logarithmic-phase cultures were prepared by initially suspending several colonies in phosphate-buffered saline (PBS, 0.1 M, pH 7.4) at a density

equivalent to a 0.5 McFarland standard of 1×10^8 colony forming units (CFU)/mL and then diluted 100 times to 1×10^6 CFU/mL. 20 µL of the diluted *P. aeruginosa* and MRSA suspension was further diluted into 60 mL cation-supplemented Mueller-Hinton (MH) broth (Oxoid) and Tryptone Soya broth (Oxoid), respectively. After culturing in the incubator at 37 ℃ for overnight, the concentration of bacteria went up to 10^8 CFU/mL again and suspensions were diluted 100 or 1000 times, yielding a starting inoculum of 10^6 CFU/mL or 10^5 CFU/mL. 10000 ppm (based on the concentration of active chlorine) stock solution of each biocide was prepared in PBS. 30 µL of each biocide solution was added into 20 mL diluted bacteria suspension, mixing thoroughly by votex to give a final concentration of 0.423 mM. Following different contact time, 1 mL samples were removed and transferred to 1 mL neutralizer solution (active chlorine was quenched by 0.02 M sodium thiosulfate ($Na_2S_2O_4$) solution and long alkyl chain was quenched by PBS buffer consisting of 1.4% [w/v] lecithin and 10% [w/v] Tween 80). Then 100 µL of bacterial suspension was taken out and diluted to 1×10^1, 1×10^2 and 1×10^3 times in sequence. Finally, 100 µL each of the bacterial suspension as well as the three diluted solutions were placed onto four zones of a Tryptone Soya agar plate (CM 0131, OXOID) and incubated at 37 ℃ for 18-20 h. The same procedure was also applied to the blanks (bacterial solution only) as controls but it was diluted to 1×10^2, 1×10^3, 1×10^4 and 1×10^5 times in sequence before plating on the agar plate.

The number of viable bacteria on 4 zones of the agar plates for the controls (A, CFU/mL) and for the biocides treated samples (B, CFU/mL) would be counted with valid counts in the range of 25-250 colonies, and the total number of bacteria was calculated using the number of viable bacteria multiplied by the dilution factor. The percentage reduction of bacteria (%) = (A-B)/A $\times$ 100; and the logarithm reduction = log (A/B). The antibacterial test of each biocide was repeated at least three times.

3.2.3.2 Uptake isotherm measurements.[121]

Final concentrations of 4.5, 9, 12, 15, 25, and 35 μg/mL of each compound (**8**, **9**, **11**, **12**) were prepared in PBS buffer (0.1 M, pH 7.4), and 4×10^{-4} M orange II dye (Sigma-Aldrich) was prepared in 0.1 M sodium chloride (NaCl) solution. 4 mL of each concentration of each compound was taken out and mixed with 1 mL prepared orange II dye solution for 5 min, followed by the addition of 5 mL chloroform to extract the dye-compound complex. The mixture was vortexed for 30 s or even longer to ensure that the chloroform and dye were mixed thoroughly. 700 μL of the chloroform phase (the bottom layer) was removed into a UV silica cuvette (VWR Spectrophotometer Cell, 10 mm light path), and the absorbance was measured at 485 nm. A PBS buffer control extracted in the same way was used to blank the spectrophotometer. Then, a standard calibration curve of each compound could be achieved by plotting the absorbance at 485 nm ($A_{485\ nm}$) *vs.* the compound concentrations.

Subsequently, 1 mL of the stock suspension (CA-MRSA/MDR *P. aeruginosa*) was added into 9 mL of each concentration of each compound, giving a final bacterial concentration of 10^9 CFU/mL. The mixture was vortexed every 20 min for a total contact time of 1 h, followed by 15 min centrifugation at 2500 RPM. 4 mL of the supernatant liquid was then removed and mixed with 1 mL orange II dye solution, and the following procedure was the same as described above. The equilibrium (unbound) concentration of compounds was calculated directly using the established calibration curves, and then the uptake concentration could be obtained by the subtraction of the initial and equilibrium concentrations. Isotherm profiles comparing the equilibrium concentration (μg/mL) with the uptake concentration (μg/10^9 cells) were plotted.

3.2.3.3 Minimal inhibitory concentration (MIC) test.

CA-MRSA and MDR *P. aeruginosa* were cultured in the broths to a concentration of 10^8 CFU/mL as described in the static antibacterial assessment. Each bacteria was diluted to 10^6 CFU/mL in the corresponding broth as the final inoculum suspension. Prepare the stock solutions of all the biocides in PBS (0.1 M, pH 7.4) and dilute (2-fold) them in broth in a 96-well plate. 100 µL of broth were added into each well as diluent and all the dilutions were prepared starting at a concentration half the stock concentration from Column 1 to Column 11. Then, 10 µL of the 10^6 CFU/mL inoculum suspension were added to each well (Column 1-11) which contained 100 µL biocide dilutions, obtaining a final bacterial concentration of 10^5 CFU/mL or 10^4 CFU/well. 10 µL inoculum were also added into well A12 containing 100 µL diluent as growth control, and well H12 (diluent only) acted as purity control. After 24 h of incubating at 37 ℃, examine the 96-well plate visually under a dark background. All the wells containing a bacterial pellet were recorded as "+" (positive) and all the clear wells as "-" (negative). Subculture the growth control well (A12) and the purity control (H12) to a Tryptic Soya agar plate to confirm the growth and purity of bacteria. Then, place the plate on the microplate reader and read it at 570 nm. The entire plate was blanked with well H12. MICs were determined to be the minimal concentration of biocides that prevented visible growth of bacteria under defined conditions.

3.2.3.4 Cytotoxicity test.

ACTT-PCS-201 neonatal human dermal fibroblasts were grown in fibroblast basal medium supplemented with fibroblast growth kit – low serum (ACTT-PCS-201-041) and incubated in 5 vol% CO_2 under humidified conditions at 37 ^{o}C. After reaching 80% confluency, the cells were trypsinized, quantified with a hemacytometer, seeded onto tissue culture-treated polystyrene 96-well plates at a final density of 10^4 cells/mL, and incubated at 37 ^{o}C for 24 h. The supernatant was then aspirated and replaced with 100 µL of either control (medium only) or compound solutions

(prepared in medium) at different concentrations. After incubation at 37 °C for 24 h, the supernatant was aspirated and replaced with 100 µL of fresh medium. Subsequently, add 10 µL of 12 mM of 3-(4,5-dimethylthiazol-2-yl)-2,5-diphenyltetrazolium bromide (MTT) stock solution, prepare by adding 1 mL of sterile PBS (0.01 M, pH 7.4) to one 5 mg vial of MTT, into each well. After a 2 h incubation at 37 °C, the supernatant was carefully removed and 50 µL of dimethyl sulfoxide (DMSO) as added to dissolve the MTT formazan crystals on the bottom. After another 10 min incubation, read absorbance at 570 nm using a microplate reader. The cell viability was calculated by taking the ratio of the absorbance of biocide treated cells to the absorbance of untreated cells.

3.2.4 Loading and releasing of synthesized biocides.

Each compound solution (0.0282 M) was prepared in PBS (0.1 M, pH 7.4) and the PAm hydrogel coated PET samples were cut into 2 × 2 cm^2. The biocide was loaded by keeping the samples in 2 mL of the compound solution at 32 ℃, 120 RPM for 90 min. The biocide loaded samples were dried at room temperature and stored in desiccator for later use. The weight increment of PET-PAm after loading was recorded, and the % of loading was determined spectrophotometrically at 485 nm after mixing with orange II dye solution and extracting with chloroform as described in section 3.2.3.2. It was calculated as %loading = $(W_0 - W_1)/W_0 \times 100$, where W_0 and W_1 was the amount of biocides in the solution before and after loading.

The release of biocides from dry PET-PAm samples was conducted at 32 ℃ in PBS at pH = 7.4. The dried, pre-loaded samples were immersed directly in the 10 mL fresh PBS at 32 ℃. Aliquots (0.5 mL) were withdrawn, diluted into 4 mL of PBS, and extracted with 5 mL of chloroform at

predetermined times to determine the concentration of biocides and, in all cases, equal volumes of PBS were immediately added to maintain a constant volume. The concentration of biocide was determined spectrophotometrically at 485 nm. Absorbance from blank (samples without drug) as a function of time was systemically measured and subtracted from the biocide-loaded samples absorbance value. The amount of biocides released from the samples in PBS, at a given time, was calculated using standard calibration curves of each biocide in PBS and expressed as percentage of total biocide content of the investigated samples. Experiments were performed in triplicate, and the average value was considered during data treatment and plotting.

Statistical Analysis: Two-sample t-test was used to check for statistical differences among the test results of the flexibility and adherence of hydrogel PET, antibacterial activity, cell viability, and biocide release. JMP software was used to determine the significant different between two curves in the time-kill profiles of biocides. Statistical significance is considered at $p \leq 0.05$.

CHAPTER 4. RESULTS AND DISCUSSION

4.1 Adherence evaluation using the wet-gelatin model.[155]

Adherence of wound dressings is one of the most important factors influencing the wound healing and regeneration. Cell adhesion test has been considered as the most popular method to evaluate the adherence of dressing materials, but it fails to reflect the real situation during wound healing. In this study, an *in vitro* easily-handled peeling model based on gelatin is adapted to evaluate the adherence of PET dressings.[103] As a proteinaceous material, gelatin can be used as an *in vitro* simulant of the *in vivo* protein-rich wound surface. Gelatin dissolves in hot water and passes from solution to gel again when cooled. This thermoreversible property makes it possible to solidify hot concentrated gelatin solution onto a fabric strip in a uniform manner, hence enabling the subsequent peeling force test with an Instron machine.

4.1.1 The peeling energy of PET dressings.

Fig. 3 plotted the peeling energies of untreated PET as a function of drying time (4 h, 6 h, 8 h, 16 h and 24 h) at two relative humidities (RHs). Initially <25% RH was used to follow the previously reported procedure.[103] As the gelatin dried out at this lower humidity, the peeling energy kept increasing rapidly with the continuous loss of water in gelatin, reaching as high as 4491.3 ± 418.8 J/m^2 after 16 h drying. After drying for 24 h, as the gelatin became more desiccated and more hardened, failure occurred within the gelatin instead of at the gelatin-dressing interface. The peeling energy results were unrealistically high and did not well simulate the clinical situation. So, we slightly adapted the reported gelatin model by drying gelatin-fabric module at a higher relative humidity. It was reported that 75% RH was the optimal for the promoting the healing of deep burns, so we chose to set the RH in the incubator at 75% RH.[122] It was found that the peeling energy also

increased with the drying time at 75% RH, but the slope of increase was much lower compared with drying at <25% RH. After drying for 4 hours at 75% RH, the peeling energy arrived at the same level (436.3 ±32.5 J/m^2) as that at <25% RH (421.3 ±52.5 J/m^2) ($p > 0.05$), but the adhesion of PET dressing increased slowly to 808.8 ±78.8 J/m^2 after 16 hours drying, only one fifth that of drying at <25% RH.

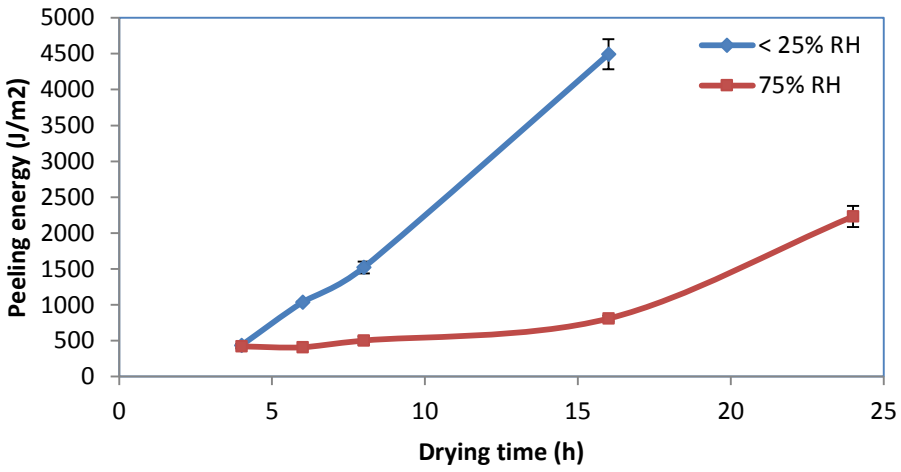

Fig. 3. Peeling energy of PET drying at different humidity (< 25% RH and 75% RH).

In this wet-gelatin model, the gelatin slab is completely hydrated at the outset, surrounded by water molecules either at a dry or moist environment. During the drying process, more and more hydrogen bonding sites of gelatin are available to the PET fabric due to the evaporation of water, so the peeling energy tends to increase with the drying time. The water loss rate of gelatin is much lower at 75% RH than at <25% RH, and the gelatin dried at 75% RH remains hydrated for longer time. Therefore, the peeling energy goes up only a little in the first 16 hours at 75% RH, when compared with a substantial increase at <25% RH. Meanwhile, gelatin is able to penetrate into the pores of PET fabric and become incorporated into fabric structure when it is solidified. This

process is similar to the clinical situation where proteinaceous exudate, newly grown capillary loops and granulation tissue penetrated into a wound dressing and became part of the dressing upon dehydration. This mechanical interlocking is considered as another factor influencing the adherence of dressing materials and varies with the degree of dryness of gelatin. When the adhesion caused by mechanical interlocking overpasses the strength of gelatin, failure occurres in gelatin itself while peeling as in the case of PET fabric/gelatin module after 24 h drying at < 25% RH.

A moisture balance of the skin tissue is achieved by constant supply from the blood circulation and drainage through the lymphatic system. In a wound, fluid leaks out of the blood vessels and white blood cells escape from the capillaries into body tissues, making up wound exudates in the early stage of the healing process. And exudate production generally reduces over time during the wound healing and regeneration. The significance of this analysis is that wound dressings adhere to a drying wound with exudates may behave in a more similar manner to the gelatin dried in a controlled moist environment 75% RH, as compared to <25% RH.

4.1.2 Effect of water/surfactant wetting on the adherence of PET dressings.

In 1982 a similar method for adherence evaluation was described by SMTL[123], involving the application of a curing silicone rubber, instead of gelatin solution, to simulate the drying of wound exudate or serum. 12 types of commercially available dressings were tested. It was found that any dressing material with the peeling energy in excess of 300-400 J/m^2 was unlikely to be a suitable primary wound dressing for a drying wound in clinical, such as Surglpad (J&J), Solvaline (Lohmann) and 32 ply gauze. In this study, even at a humid environment of 75% RH, the peeling energy of PET dressing after 24 h drying still reached as high as 2231.3 ± 296.3 J/m^2 (Fig. 4), approximately 5 times higher than the above limit. Water has been identified as the principal

element in debonding adhesives and substrates. In clinical situations, water or surfactant solution is always used to moisten wound dressings prior to detachment. After drying for 24 h at 75% RH, 500 μL DI water or foaming surfactant (2% chlorhexidine gluconate solution, Hutington) was added onto the surface of PET and allowed to penetrate into the interface between gelatin and the fabric for 1 min, 5 min and 10 min before the peeling force test. As we can see from Fig. 4, the peeling energy dropped drastically from 2231.3 ±296.3 J/m^2 to 481.3 ±87.5 J/m^2 and 446.0 ±43.8 J/m^2 after 1 min of water and surfactant treatment, respectively. Gelatin has an extremely low water content after 24 h drying. Additional water molecules can permeate and migrate to the gelatin-dressing interface, replacing PET to re-form hydrogen bonds with the dehydrated gelatin and thus largely easing the peeling.[124-5] However, there was no further decrease with the extended water/surfactant treatment time before the peeling force test. And no significant difference was notified between the effects of water and surfactant solution ($p>0.05$), even though surfactant is known to aid the wetting of hydrophobic surfaces. It indicates that 500 μL of water can fully swell the interface with an area of 16 ×60 mm^2 within 1 min, achieving maximal debonding.

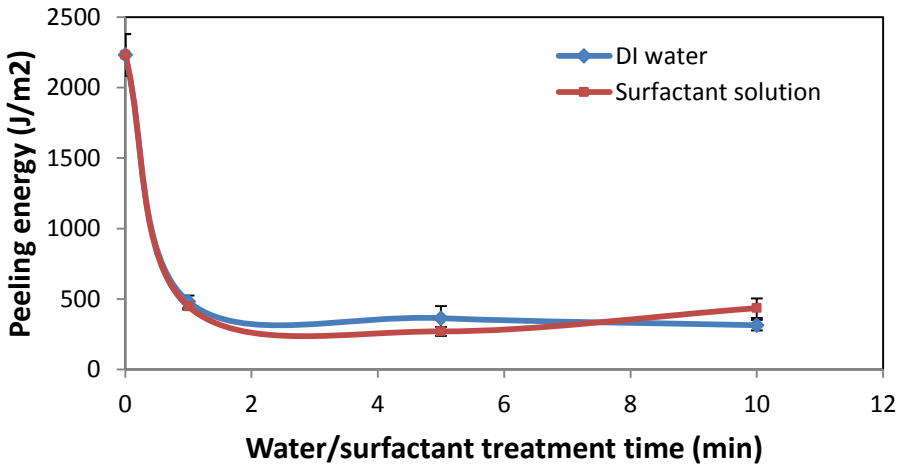

Fig. 4. Peeling energy of PET dressings wetted with water/surfactant before peeling.

4.2 Deposition of PAm hydrogel on PET dressings.[155]

As early as 1988, W. Pekala *et al.*[126] published the patent describing a method of manufacturing hydrogel dressings by radiation cross-linking and brought to the local market in 1992. Photopolymerization has been widely used to convert a liquid monomer or macromere to a hydrogel by free radical polymerization, which is one of the most convenient and fast methods in the production of hydrogels.[92] In this study, a thin layer of PAm hydrogel was grown from the surface of O_2 plasma treated PET fabric under UV irradiation via the "sandwich" method. O_2 plasma treatment was used generate peroxides on the surface of PET fabric, which degraded upon UV irradiation to generate radicals for surface initiated crosslinking copolymerization of AM and MBA. Three irradiation durations were used and the corresponding sample denotation and weight increment were listed in Table 1. The amount of deposited hydrogel increased with the increasing UV irradiation time. 30 min UV irradiation was not long enough to form well-crosslinked hydrogel on PET fabrics. PET-PAm-II and PET-PAm-III were further characterized in terms of their hydrophilicity, water swelling capacity and adherence.

Table 1. Hydrogel deposition on PET as a function of UV irradiation time.

Sample denotation	PET-PAm-I	PET-PAm-II	PET-PAm-III
UV irradiation time	30 min	50 min	70 min
Weight increment	0	5.81% ± 1.56%	10.21% ± 0.71%

4.2.1 Characterization of PAm hydrogel deposited on PET.

In Fig. 5, the peak at ~1717 cm^{-1} in the attenuated total reflectance–fourier transform infrared spectroscopy (ATR-FTIR) spectrum of PET attributed to the stretching absorption of C=O in the ester bond, while the absorbance of this peak declined steadily after 50 min and 70 min UV irradiation, indicating that the PET substrate has been covered by hydrogel during the polymerization. In the PET-PAm hydrogel spectrum, peaks in the region of 3186-3364 cm^{-1} could be assigned to the stretching vibration of N-H; the peaks at ~1650 cm^{-1} and ~1610 cm^{-1} corresponded to amide I (C=O) and amide II (N-H) in PAm, respectively. Moreover, the peaks of amide in PAm got higher with the prolonged light exposure time, suggesting larger amount of hydrogel on PET fabrics.

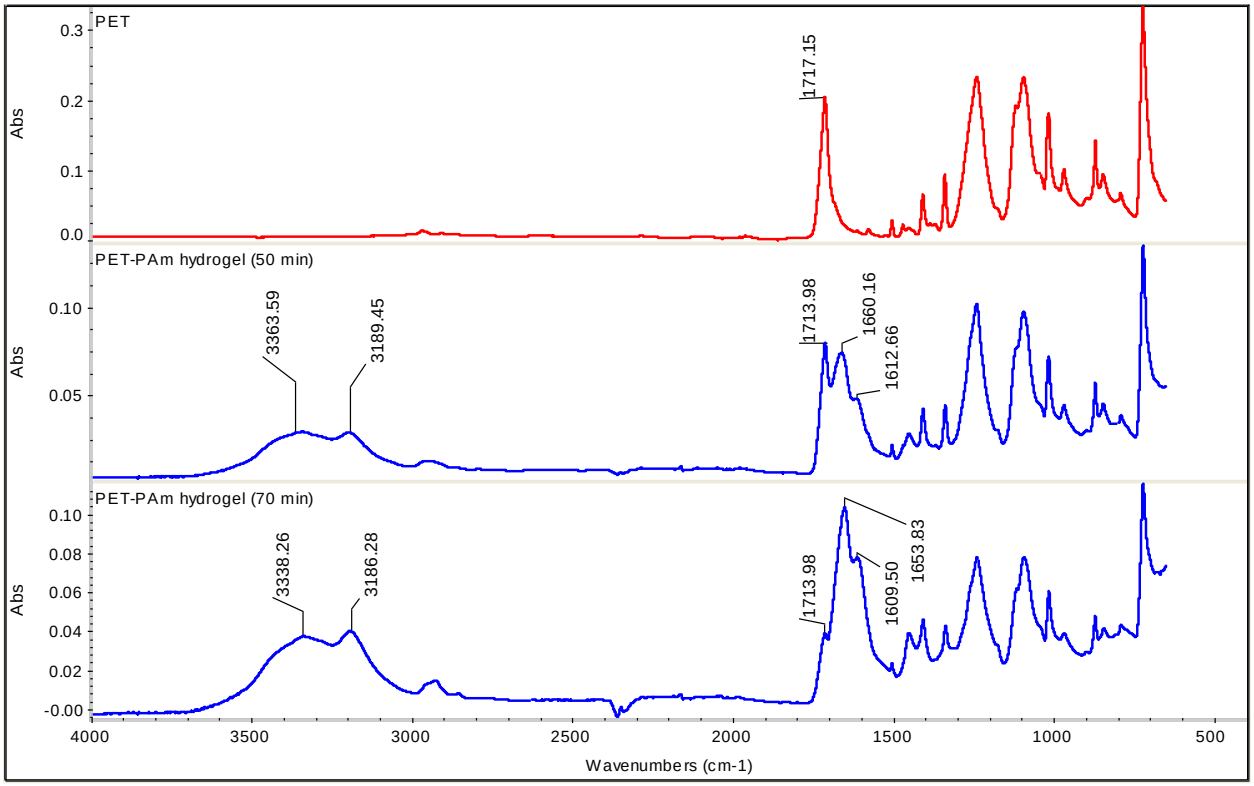

Fig 5. ATR-FTIR spectra of samples.

Water contact angle measurement was used to characterize the hydrophilicity of the PAm hydrogel layer on the PET surface because the crosslinked PAm hydrogel was highly water-absorbent. As shown in Fig. 6, the initial water contact angle for untreated PET fabric was about 127 °because of the hydrophobic structure of the ester group in the PET chain. After the photopolymerization, it decreased to 77 °and 56 °for PET-PAm-II and PET-PAm-III, respectively. After 5 min, the water contact angle for PET decreased by only 4 °, whereas the water contact angle for PET-PAm-II and PET-PAm-III turned to 30 °and 21 °, respectively, and further decreased to 0 °after 20 min for the PET-PAm-III. The results of ATR-FTIR and water contact angle measurement suggest that PAm hydrogel has been successfully deposited onto the PET dressing via the plasma induced graft polymerization.

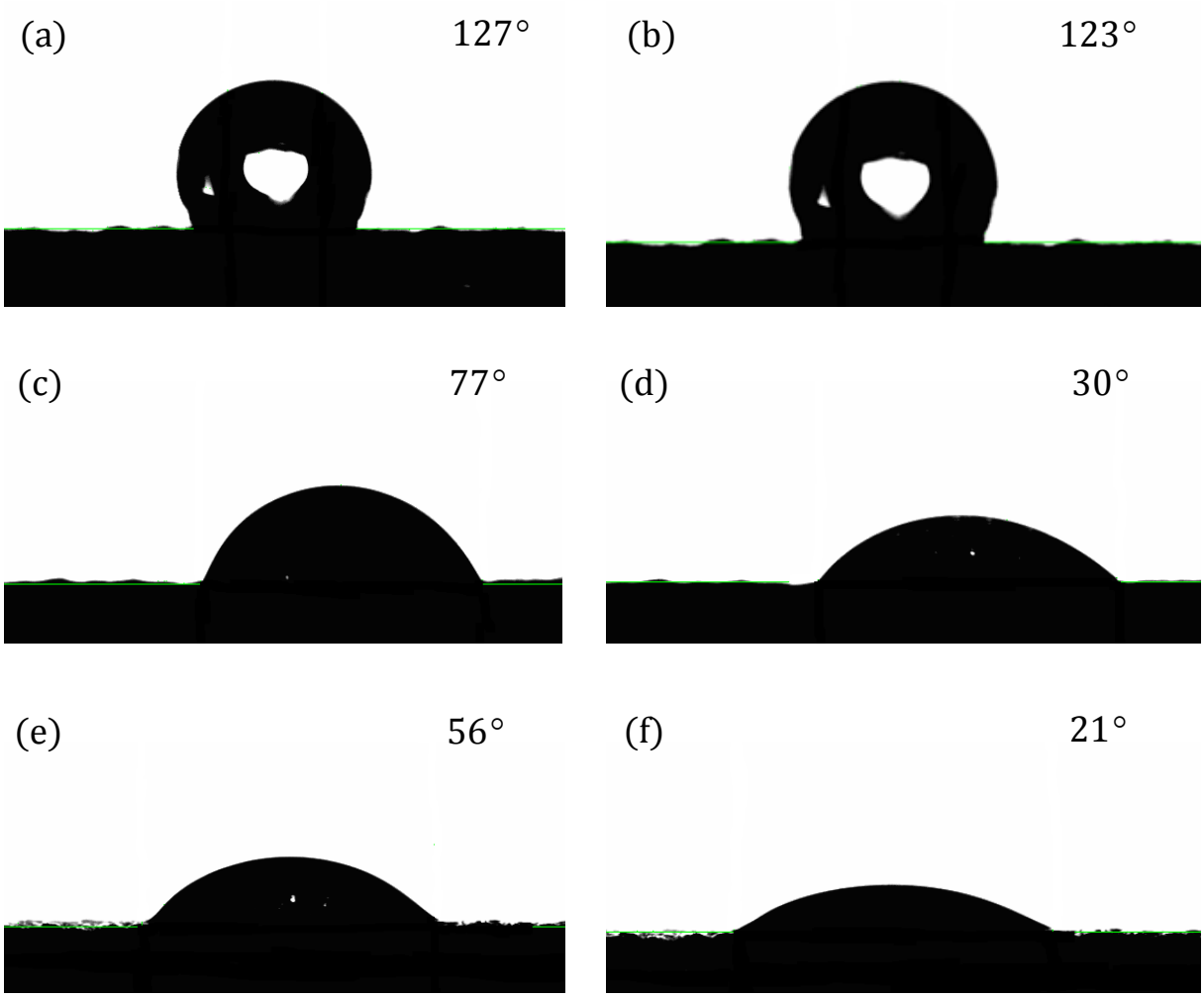

Fig. 6. Water contact angle of PET after (a) 0 min and (b) 5 min; and of PET-PAm-II after (c) 0 min and (d) 5 min; and of PET-PAm-III after (e) 0 min and (f) 5 min.

4.2.2 Swelling ratio of PET dressings after the deposition of PAm hydrogel.

Before the peeling force test, all the samples were immersed in DI water and allowed to swell at room temperature. The swelling process was investigated by means of weighing test and the ability for swelling was called "swelling ratio", which was closely relevant to its ability to retain moisture. From Fig. 7, one can see that the swelling ratio of PET-PAm-II and PET-PAm-III reached as high as 77.18% ± 2.10% and 155.58% ± 9.86%, respectively, as compared to that of untreated PET with merely 11.11% ± 0.72%. PAm polymers are long parallel chains of molecules and when crosslinked they can create a three-dimensional network of polymeric chains. Water is brought into the network through the process of osmosis and quickly journeys into the central part of the polymer network.[19, 91] Then the three-dimensional network of PAm reserves the water and appears as the gel. Hydrogels are capable of absorbing up to 500 times their original weight in water. As shown in Table 1, the amount of crosslinked PAm hydrogel on PET-PAm-III (10.21% ± 0.71%) was almost twice as much as that on PET-PAm-II (5.81% ± 1.56%), which could help explain why the swelling ratio of PET-PAm-III was far more than that of PET-PAm-II.

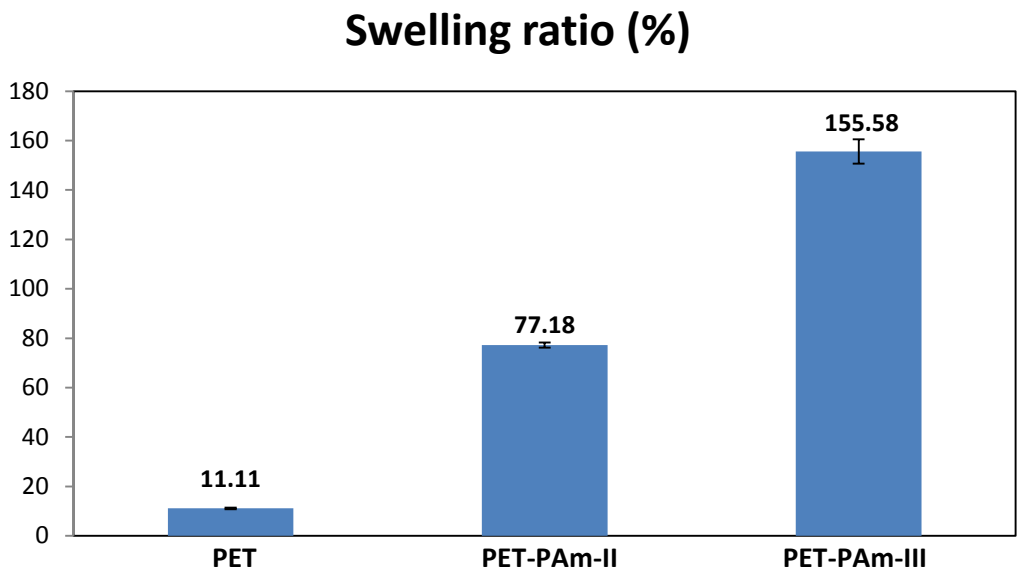

Fig. 7. Swelling ratios of untreated PET, PET-PAm-II and PET-PAm-III.

4.2.3 Adherence of PET dressings after the deposition of PAm hydrogel.

Typically, the frequency of dressing changes should be at least 1 day. We previously stated that samples dried at a higher humidity was more closed to the real situation for wound healing. So the hydrogel coated PET fabrics were dried in the incubator at 32 ^{o}C, 75% RH for 24 h before the peeling test. After the deposition of hydrogel, the peeling energy of PET fabric dropped from 2231.3 $\pm$ 296.3 J/m^2 to lower than 300 J/m^2 as can be seen in Fig. 8, which is closely relevant to the swelling capacity of hydrogels. The hydrophilic property enables hydrogels to absorb plenty of water and to retain it within the three-dimensional structure. When the surroundings begin to dry out, the crosslinked hydrogel can gradually dispense up to 95% of the stored water.[130] This process of rehydration and dehydration of hydrogel can be repeated for many times to maintain an optimal moisture balance. In this study, hydrogel coated PET dressings were allowed to swell in water for 5 min before the peeling force test, taking in a large amount of water. During the drying

process, gelatin tended to become hard and desiccated while the PAm hydrogel on PET could donate water to keep the gelatin hydrated. Thus, the hydrogen bonding sites of gelatin were always surrounded by water molecules and unavailable for bonding to the fabric surface, producing a much lower peeling energy even after drying for 24 h. There was NO significant difference between the peeling energy of PET-PAm-II and PET-PAm-III ($p>0.05$) even though PET-PAm-III had a higher water swelling capacity. Therefore, this hydrogel layer do help ease the peeling of PET dressings, however, another concern will raise up about the flexibility of PET after the deposition of hydrogel.

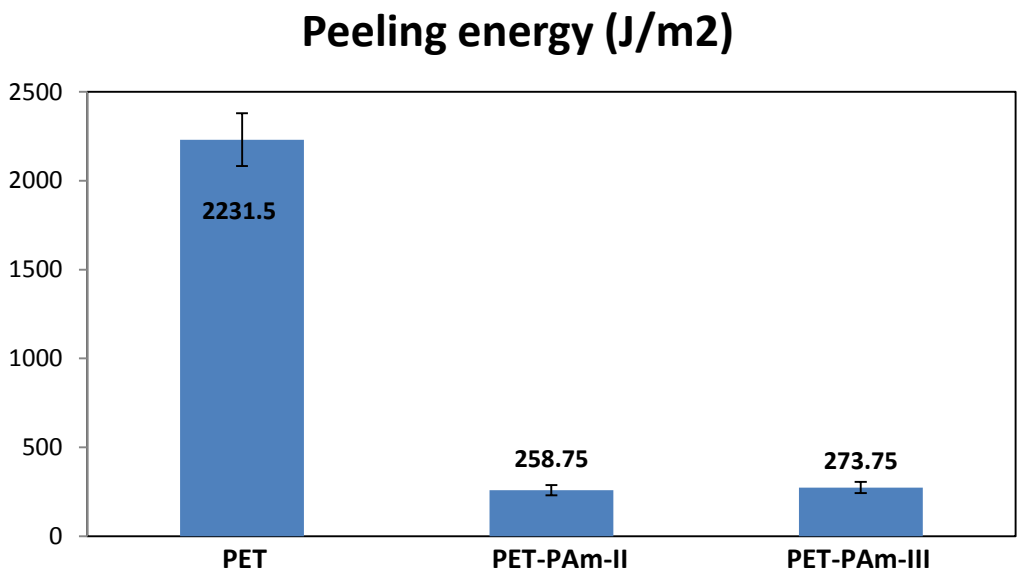

Fig. 8. Peeling energy of untreated PET, PET-PAm-II and PET-PAm-III.

4.2.4 Flexibility of PET dressings after the deposition of PAm hydrogel.

Flexibility is an important performance parameter of wound dressings, influencing their ability to conform to the body shape and form an intimate contact with the wound. If the dressings are very poorly conformable, they may quickly detach when body movement occurs. Sometimes it is also

difficult to apply wound dressings to the body parts with some irregular contours and shapes. The flexibility and conformability of a wound dressing is essential to ensure its effectiveness for wound healing in different manners. It can help maintain a moist environment at the wound-dressing interface by absorbing and retaining the wound fluid, and no fluids will spread to the peri-wound skin, thereby reducing the possibility of maceration.[127] It contributes to preventing blisters and improving patient comfort by minimizing the shear forces of wound dressings and allowing greater mobility for patients.[128] It is also conductive to avoid "dead space" where bacteria can accumulate and proliferate, and thus to ensure the highly efficient delivery of the bactericides incorporated in dressings.[70]

Flexibility was tested by measuring the overhang length recommended by ASTM standard D 1388-96 as the sample gravitationally bended under its own weight.[119] Flexural rigidity is defined as the resistance to bending, which is a measure of the interaction between the sample weight and its bending stiffness. PET is well-known for its excellent flexibility and conformability as the representative material of wound dressings, and the flexural rigidity of wet untreated PET fabric was merely 7.40 mg•cm (Table 2). After the deposition of hydrogel, the flexural rigidity increased to 17.02 mg•cm and 13.19 mg•cm for wet PET-PAm-II and PET-PAm-III, respectively. It has been reported that the flexural rigidity of a strong yet drapeable non-woven fabric with a very attractive handle is 40 mg•cm, and fabrics with the flexural rigidity of 154 mg•cm can be used as bed sheets, underwear and a substrate for a coated fabric for rainwear.[129] Although the flexural rigidity of the untreated PET fabric slightly increased after the deposition of hydrogel, PET-PAm samples could still well conform to body contours as shown in Fig. 9. Therefore, the thin layer of PAM hydrogel grown from the PET substrate via a "sandwich" method does not significantly compromise the flexibility of the PET fabric.

Table 2. The flexural rigidities of PET, PET-PAm-II and PET-PAm-III.

Sample denotation	PET	PET-PAm-II	PET-PAm-III
Overhang length (o)	1.55 ± 0.02 cm	1.70 ± 0.00 cm	1.56 ± 0.00 cm
Bending length (c)	0.78 cm	0.85 cm	0.78 cm
Fabric mass per unit area (W)	15.00 mg/cm^2	27.71 mg/cm^2	27.79 mg/cm^2
Flexural rigidity (G)	7.12 mg•cm	17.02 mg•cm	13.19 mg•cm

Fig. 9. Images of PET-PAm dressings applied to different body parts.

4.3 Study of new "composite" biocides.

We previously reported the synthesis the 5,5-dimethyl hydantoin (DMH) analog (compound **1**) that contains one DMH moiety and one QA salt moiety.[67] In this project, we prepared a series of new DMH analogs with multiple QA cationic moieties as well as long-chained QAs to explore the corresponding further boosting effect or possible synergetic effect. The chemical synthesis is depicted in Scheme 3. DMH bromide **13** was prepared according to our previously published procedure. Reacting the large excess commercially available *N,N,N',N'*-Tetramethylethylenediamine with bromide **13** under reflux conditions gave the QA-tertiary amine

14 as white solid. We completed the quaternization of the structural terminal tertiary amine by treating **14** with excess MeI at room temperature. By passing **14** through an ion exchange resin, we then obtained compound **3 (**Cl- form of **14**) which could be chlorinated using t-BuOCl to give **6**. DMH abutted with tertiary amine (**15**) was produced by reacting bromide **13** with excess dimethyl amine. Following quaternization of **15** with **13** smoothly afforded the product **2**. Similar quaternization with different alkyl bromides yield QA products **7-9** containing long alkyl chains that may render antibacterial activity. All these synthetic QA compounds, including **2**, **7-9**, were transformed into corresponding Cl^- form before the chlorination step to give the new "composite" biocides with both *N*-chloramide and QA moieties: **5, 10-12**. The ratios of *N*-chloramide versus QA moiety moiety in compounds **4**, **5** and **6** are 1, 2 and 0.5, respectively. All the compounds were characterized with NMR.

4.3.1 Static antibacterial efficacy.

MRSA and MDR *P. aeruginosa* have become two of the most frequently isolated organisms in burn wounds, thus, they are selected as the microbes to evaluate the antibacterial performance of the synthesized compounds.[131] According to our previous study, compound **4** of dimethyl-hydantoin (DMH) based *N*-chloramide covalently linked with a positively charged, short-chained QA moiety (1:1) exhibited more efficient antibacterial activity, as compared to *N*-chloramide alone. Herein we sought to study the effect of the ratio of QA moiety/*N*-chloramide on the bactericidal efficacy and we envisaged that multiple QA moieties with the ratio of 2:1 (compound **6**) would further improve the biocidal property. Compound **5** with the ratio of 0.5:1 of QA moiety to *N*-chloramides was also synthesized to serve as a reference. We speculated that the bactericidal efficacy increased with the increasing ratio of QA moiety/*N*-chloramide due to the stronger electrostatic interaction with negatively charged bacterial cells. On the other hand, it is well-known

that the relative antibacterial efficiency of QA salts significantly depends on the alkyl chain length, following an approximate parabolic function peaking at C_{12-14} for gram-positive bacteria and C_{14-16} for gram-negative bacteria.[46] The effect of alkyl chain length of QA moiety (compound **10-12**) on the antibacterial activity was also investigated in this study, anticipating a synergistic effect between *N*-chloramide and long-chained QA moiety. Prior to evaluating the antibacterial activity of the final products, the efficacy of the non-chlorinated precursors (compound **1-3**, **7-9**) was evaluated to fully understand the benefit of designing a combination approach.

Compounds **1-6** with short-chained QA moieties at the concentration of 0.423 mM (or 15 ppm of [Cl+] for *N*-chloramides) were challenged with 10^6 CFU/mL of MRSA and MDR *P. aeruginosa,* providing time-kill profiles for each compound. As it can be seen from Table 3, no discernible antibacterial activity was detected at the chosen concentration of non-chlorinated precursors **1-3** with short alkyl chain. The antibacterial function of short-chained QA salts mainly results from the attractive interactions with the negatively charged cell to form a surfactant-microbe complex. It causes the disruption of essential membrane functions, and thus the degradation of proteins and nucleic acids, resulting in a loss of multiplication ability of bacterial cells.[46-8] All the above actions require long periods of contact. The contact time of 60 min appears to be too short for the short-chained QA salts to manifest any detectable bactericidal effect. Conversely, the chlorinated counterparts **4-6** exerted considerable killing efficiency against 10^6 CFU/mL of MRSA, achieving more than 99.55% (2.35-log) bacterial reduction at 60 min. However, there was no effective inactivation of 10^6 CFU/mL of MDR *P. aeruginosa*. Thus, the inoculum concentration of *P. aeruginosa* was decreased to 10^5 CFU/mL and difference contact time were chosen as listed in Table 4, arriving at a total killing after 1 h.

For these "composite" compounds **4-6**, *N*-chloramide, rather than QA cationic center, is considered as the primary cause of bacterial death within the studied time frame. The killing mechanism of *N*-chloramide involves the entire molecular structure, not the limited amount of free chlorine produced in the hydrolysis equilibrium.[133] After approaching bacterial cells, *N*-chloramide starts the attack by means of chlorination of the external protein matrix to form a chlorine cover; meanwhile, *N*-chloramide molecule penetrates into the intact bacteria, targeting at the vital sites mainly S-H and S-S groups in proteins via irreversible oxidation of active chlorine.[66] Gottardi[132] found that the determining killing rate of *N*-chloramines within the short period of contact time was the slow penetration into intact cells, instead of the extent of the relatively fast surface chlorination. It serves as evidence for the importance of penetration of *N*-chloramines, which is strongly dependent on the cell accessibility to the biocides. Gram-negative *P. aeruginosa* was proved to be less sensitive to compound **4-6** than gram-positive MRSA, which might be attributed to the rigid outer membrane. The lipopolysaccharide outer membrane of *P. aeruginosa* is likely to offer a hindrance for the penetration of *N*-chloramides into cells, contributing to a higher intrinsic resistance to this mechanism of antibacterial activity.[43, 134-5]

No significant difference existed in the time-kill profiles ($p > 0.05$) of compounds **4**, **5**, and **6** with different ratios of QA moiety/*N*-chloramide against both tested microbes. However, the bacterial reduction of compound **5** with the lowest ratio of 0.5/1 resulted in only 70.81% (0.54-log) reduction against 10^5 CFU/mL of MDR *P. aeruginosa* at 20 min, significantly ($p < 0.05$) lower than 99.65% (2.46-log) and 99.67% (2.50-log) reduction achieved by **4** and **6**, respectively. The higher bulk and hydrophobicity of compound **5** might slow down its diffusion rate into intact cells through the water-filled porins in the lipidic outer membrane of *P. aeruginosa*. There was no further acceleration in the killing kinetics of compound **6** with an additional cationic QA center

(the ratio of 2/1). The cell accessibility for the penetration of biocides, rather than the ionic interaction for the approach, plays the pivotal role in the antibacterial activity.

Table 3. Antibacterial results of compound **1-7, 10** against 10^6 CFU/mL of MRSA and MDR *P. aeruginosa.*

Synthetic compounds		Bacterial Reduction at Various Contact Time (min)				
		1	**3**	**5**	**10**	**60**
Gram-positive MRSA (10^6 CFU/mL)*						
1-3,7	%	NO antibacterial activity				
	Log_{10}					
4	%	82.94 ± 0.20	91.86 ± 0.90	86.12 ± 0.50	93.03 ± 1.16	99.88 ± 2.93
	Log_{10}	0.77 ± 0.01	1.09 ± 0.05	0.86 ± 0.02	1.16 ± 0.02	2.93 ± 0.02
5	%	91.54 ± 1.35	91.43 ± 1.10	87.22 ± 0.95	89.13 ± 0.65	99.55 ± 0.04
	Log_{10}	1.08 ± 0.07	1.07 ± 0.06	0.89 ± 0.03	0.96 ± 0.03	2.35 ± 0.04
6	%	93.66 ± 0.25	93.06 ± 0.30	90.97 ± 0.25	91.75 ± 0.35	99.56 ± 0.06
	Log_{10}	1.20 ± 0.02	1.16 ± 0.02	1.04 ± 0.01	1.08 ± 0.02	2.36 ± 0.06
10	%	78.26 ± 1.48	78.86 ± 0.04	82.81 ± 1.90	89.27 ± 0.47	98.80 ± 0.34
	Log_{10}	0.66 ± 0.03	0.67 ± 0.00	0.76 ± 0.05	0.97 ± 0.02	1.93 ± 0.12
Gram-negative MDR *P. aeruginosa* (10^6 CFU/mL)*						
1-3	%	NO antibacterial activity				
	Log_{10}					
4	%	21.84 ± 6.18	26.21 ± 10.98	21.36 ± 6.87	41.26 ± 4.81	10.68 ± 0.05
	Log_{10}	0.11 ± 0.03	0.13 ± 0.06	0.11 ± 0.04	0.21 ± 0.06	0.08 ± 0.04
5	%	-5.34 ± 32.27	5.83 ± 6.87	8.74 ± 0.00	10.19 ± 0.69	14.08 ± 8.92
	Log_{10}	-0.01 ± 0.14	0.03 ± 0.03	0.04 ± 0.00	0.05 ± 0.00	0.07 ± 0.05
6	%	38.83 ± 1.37	37.86 ± 4.12	31.55 ± 3.43	25.73 ± 2.06	26.21 ± 1.37
	Log_{10}	0.21 ± 0.01	0.21 ± 0.03	0.16 ± 0.02	0.13 ± 0.01	0.13 ± 0.01

*****Inoculum concentration of MRSA and MDR *P. aeruginosa* was 1.62×10^6 CFU/mL and 2.06×10^6 CFU/mL, respectively.

Table 4. Antibacterial results of compound **1-7, 10** against 10^5 CFU/mL of MDR *P. aeruginosa.*

Gram-negative MDR *P. aeruginosa* (10^5 CFU/mL)**	
	Bacterial Reduction at Various Contact Time (min)

Synthetic compounds		3	10	20	30	60
1-3,7	%	NO antibacterial activity				
	Log_{10}					
4	%	37.61 ± 1.88	61.50 ± 1.88	99.65 ± 0.00	99.99 ± 0.00	100 ± 0.00
	Log_{10}	0.20 ± 0.01	0.41 ± 0.02	2.46 ± 0.02	4.02 ± 0.21	5.35 ± 0.00
5	%	22.57 ± 4.38	26.55 ± 12.52	70.81 ± 5.22	99.96 ± 0.02	100 ± 0.00
	Log_{10}	0.11 ± 0.02	0.14 ± 0.07	0.54 ± 0.08	3.36 ± 0.25	5.35 ± 0.00
6	%	39.82 ± 10.01	62.83 ± 1.25	99.67 ± 0.12	100 ± 0.00	100 ± 0.00
	Log_{10}	0.22 ± 0.07	0.43 ± 0.01	2.50 ± 0.17	4.82 ± 0.92	5.35 ± 0.00
10	%	42.68 ± 0.67	49.34 ± 16.39	68.56 ± 3.59	97.00 ± 0.61	100 ± 0.00
	Log_{10}	0.24 ± 0.01	0.31 ± 0.14	0.50 ± 0.05	1.52 ± 0.09	5.80 ± 0.00

******Inoculum concentration of MDR *P. aeruginosa* was 2.26×10^5 CFU/mL for **1**-**6** and 2.98×10^5 CFU/mL for **7**, **10**.

The bactericidal efficacy of QA salts exhibits a strong dependence on the alkyl chain length, but there was still no detectable bacterial reduction in this study even after increasing the length from methyl group (compound **1**) to hexyl group (compound **7**). Hexamer was reported to show characteristically slower disinfection rates by crossing intact cell membrane and inhibiting protein and DNA activities.[136] The killing kinetics of compound **10** (chlorinated **7**) was even slower than compound **4**, especially against MRD *P. aeruginosa*, arriving at merely 1.52-log reduction after 30 min in comparison with 4.02-log reduction of **4** as listed in Table 4. It can be well explained that the penetration into pathogens is favored for *N*-chloramides with lower bulk. Thus, the combination of *N*-chloramide with hexyl group has no synergistic, but antagonistic effect in the antibacterial activity. Further increasing the alkyl chain length to dodecyl **11** and tetradecyl **12** resulted in an instantaneous total killing of 10^6 CFU/mL of both microbes, therefore, the inoculum concentration was raised up to 10^7 CFU/mL (Table 5). 7.05-log and 7.55-log reduction of MRSA was achieved by compound **11** and **12** at 5 min, respectively, while 5.57-log and 7.50-log reduction of MDR *P. aeruginosa* within 90 min. Long-chained QA salts endow the "composite" biocides

with an additional killing mechanism by inserting into membrane lipid domains of bacteria, inducing physical disruption and rapid inactivation. [46-7, 137] Longer alkyl chain shows more potent bactericidal efficacy due to deeper insertion.

In order to study the possible synergistic effect of the "composite" biocide (**11** or **12**), the mixture of separate *N*-chloramide (**4**) and long-chained QA salt (**8** or **9**) was also formulated at equal dose of 0.423 mM for each, marked as **4+8** or **4+9**. Compound **4** is chosen as the *N*-chloramide counterpart of the "composite" biocides to ensure that both components in this formulation (**4+8** or **4+9**) are endowed with a cationic center. Time-kill profiles in Fig.10 were plotted using the data in Table 5 for better comparative purposes. There was only 0.93-log (88.21%) reduction of 10^7 CFU/mL of MRSA achieved by the *N*-choramide precursor dodecyl **8** within 90 min. The formulation of **4+8** provided a much more favorable killing efficiency, arriving at 7.05-log (100%) reduction at 60 min, and there was a further enhancement of "composite" compound **11** with a complete elimination within only 5 min. Smaller differences were noted in the batch of tetradecyl **9**, **12** and **4+9**, but the trend in the antibacterial activity was accordant. Compound **9** with long chain alone exerted the least remarkable bacterial efficacy. No significant difference existed in the killing kinetics of compound **12** and compound **4+9** ($p > 0.05$). However, compound **12** achieved a total killing of 7.55-log bacterial reduction at 5 min, as compared to 6.95-log of compound **4+9** ($0.05 < p < 0.1$). Covalently combining *N*-chloramide and long-chained QA moieties was proved advantageous with the fastest disinfection kinetics, indicating a synergistic effect of these two components against MRSA. Conversely, compound **8** had the best killing against MDR *P. aeruginosa* during the first 10 min, achieving the maximum of approximately 2-log reduction. The bacterial reduction of chlorinated **11** slowly increased to 1.88-log reduction at 10 min and exceeded that of compound **8**, arriving at 5.57-log reduction after 90 min. Similarly, compound **9** had a faster

killing kinetics with a total killing of 7.50-log reduction at 30 min, as compared to 6.63-log of compound **12**. The mixture of **4+8** and **4+9** exhibited the worst antibacterial performance against *P. aeruginosa*. The disparity in the time-kill profiles of the biocides might imply different modes of action against these two microbes.

Table 5. Antibacterial results of dodecyl **8**, **11**, **4+8** and tetradecyl **9**, **12**, **4+9** against 10^7 CFU/mL of MRSA and MDR *P. aeruginosa*.

Gram-positive MRSA (10^7 CFU/mL)***								
Synthetic compound		Bacterial Reduction at Various Contact Time (min)						
		1	**3**	**5**	**10**	**30**	**60**	**90**
8	%	26.79 ±5.50	22.32 ±5.68	56.25 ±3.79	55.36 ±5.41	58.93 ±8.84	77.23 ±1.89	88.21 ±0.25
	Log_{10}	0.14 ±0.03	0.11 ±0.03	0.36 ±0.04	0.36 ±0.05	0.41 ±0.10	0.64 ±0.04	0.93 ±0.01
11	%	99.97 ±0.00	100 ±0.00	100 ±0.00	100 ±0.00	100 ±0.00	100 ±0.00	100 ±0.00
	Log_{10}	3.52 ±0.01	5.44 ±0.00	7.05 ±0.00	7.05 ±0.00	7.05 ±0.00	7.05 ±0.00	7.05 ±0.00
4+8	%	16.31 ±4.68	23.60 ±0.00	68.11 ±2.80	99.97 ±0.00	100 ±0.00	100 ±0.00	100 ±0.00
	Log_{10}	0.07 ±0.02	0.12 ±0.00	0.50 ±0.04	3.54 ±0.04	5.20 ±0.34	7.05 ±0.00	7.05 ±0.00
9	%	99.97 ±0.00	100 ±0.00	100 ±0.00	100 ±0.00	100 ±0.00	100 ±0.00	100 ±0.00
	Log_{10}	3.53 ±0.02	4.79 ±0.11	5.19 ±0.44	6.42 ±0.59	7.55 ±0.22	7.55 ±0.22	7.55 ±0.22
12	%	99.99 ±0.01	100 ±0.00	100 ±0.00	100 ±0.00	100 ±0.00	100 ±0.00	100 ±0.00
	Log_{10}	4.93 ±0.91	7.11 ±0.29	7.55 ±0.22	7.55 ±0.22	7.55 ±0.22	7.55 ±0.22	7.55 ±0.22
4+9	%	99.97 ±0.01	100 ±0.00	100 ±0.00	100 ±0.00	100 ±0.00	100 ±0.00	100 ±0.00
	Log_{10}	3.54 ±0.05	6.42 ±0.31	6.95 ±0.41	7.55 ±0.22	7.55 ±0.22	7.55 ±0.22	7.55 ±0.22
Gram-negative MDR P. aeruginosa (10^7 CFU/mL)***								
		1	**3**	**5**	**10**	**30**	**60**	**90**
8	%	74.27 ±8.47	96.70 ±1.99	98.60 ±0.73	98.61 ±0.81	99.19 ±0.29	99.33 ±0.22	99.33 ±0.20
	Log_{10}	0.70 ±0.22	1.73 ±0.29	2.07 ±0.29	2.10 ±0.29	2.21 ±0.22	2.28 ±0.21	2.26 ±0.19
11	%	34.54 ±3.81	80.36 ±5.59	89.37 ±1.76	93.91 ±0.39	99.90 ±0.05	99.99 ±0.01	100 ±0.00
	Log_{10}	0.19 ±0.03	0.75 ±0.12	0.99 ±0.07	1.88 ±0.12	3.17 ±0.25	4.13 ±0.18	5.57 ±0.75
4+8	%	16.31 ±4.68	23.60 ±0.00	68.11 ±2.80	99.97 ±0.38	98.10 ±0.19	98.74 ±0.15	98.84 ±0.40
	Log_{10}	0.07 ±0.02	0.12 ±0.00	0.50 ±0.04	1.22 ±0.03	1.73 ±0.05	1.91 ±0.05	2.00 ±0.14
9	%	98.99 ±0.45	99.97 ±0.02	100 ±0.00	100 ±0.00	100 ±0.00	100 ±0.00	100 ±0.00
	Log_{10}	2.11 ±0.19	4.30 ±0.53	5.79 ±0.86	6.43 ±0.41	7.50 ±0.17	7.50 ±0.17	7.50 ±0.17
12	%	97.82 ±0.87	99.94 ±0.05	99.99 ±0.01	100 ±0.00	100 ±0.00	100 ±0.00	100 ±0.00
	Log_{10}	1.75 ±0.16	3.82 ±0.45	4.60 ±0.52	5.39 ±0.31	6.63 ±0.33	7.50 ±0.17	7.50 ±0.17
4+9	%	97.15 ±1.11	99.92±0.04	99.99 ±0.01	100 ±0.00	100 ±0.00	100 ±0.00	100 ±0.00
	Log_{10}	1.69 ±0.24	3.29 ±0.27	4.08 ±0.26	4.66 ±0.12	4.91 ±0.34	5.58 ±0.24	6.13 ±0.55

*******Inoculum concentration of MRSA and MDR *P. aeruginosa* was in the range of 1.07-5.29 × 10^7 CFU/mL and 1.55-7.90 × 10^7 CFU/mL, respectively.

[#]**4**+**8** and **4**+**9** represents the mixture of separate biocides **4** and **8** or **9** with the same dose of 15 ppm for each.

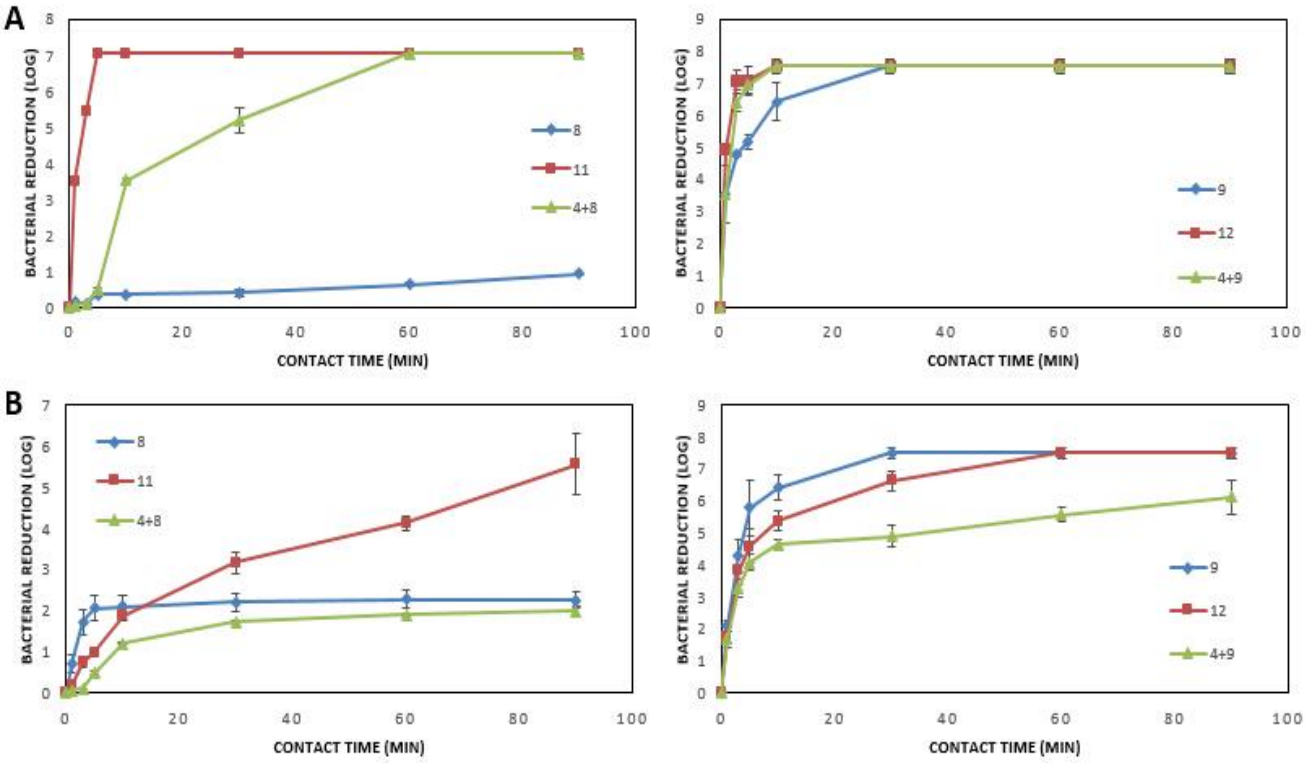

Fig. 10. Bacterial reduction (log) as a function of contact time between biocides and bacteria: (A) 1.07-5.29 × 10^7 CFU/mL of MRSA; (B) 1.55-7.90 × 10^7 CFU/mL of MDR *P. aeruginosa*. All the time-kill profiles are significant different except for the killing kinetics against MRSA (A) between the mixture of compound **4**+**9** and compound **9** or **12**.

The interaction of a biocide with a given cell is conventionally measured by etermining its adsorption, providing estimable information on the availability of target sites. To identify the differences in the mode of action of compound **8-12** against MRSA and MDR *P. aeruginosa*, the uptake isotherms of each compound was obtained via a spectrophotometric method.[121] Uptake isotherms record the amount of biocide bound to (absorbed by) cells versus the unbound

(equilibrium) concentration of biocide. This method depends on the one-to-one specific binding between an anionic dye, Orange II, and QA salts. The dye-salt complexes can be spectrophotometrically determined after chloroform extraction from aqueous solution so that quantification of QA salt adsorbed by bacterial cells can be obtained. To avoid multiple antibacterial effects at high concentrations of biocides, low concentrations were used to single out the prime lesion of biocide adsorption to cell membrane. Based on the uptake classification scheme developed by Giles[138], all the uptake isotherms in Fig. 11 followed the Langmuir (L) pattern but different subclass groups, where the adsorption of biocides become more difficult due to the decreasing vacant binding sites with the progressive covering of the bacterial membrane. Overall, the uptake of tetradecyl **9** was almost two to three times that of dodecyl **8**, that is, the uptake of biocides by cells increased with the increasing length of alkyl chain of the QA moiety. Longer chain has a higher binding affinity to the cell membrane due to its higher lipophilicity and thus giving a much faster inactivation kinetics. The isotherm profiles of all test compounds by MRSA belonged to L3 pattern as shown in Fig. 11 (A). Both dodecyl compound **8** and **11** had an inflection point in the uptake isotherms, which might be attributed to additional binding sites arising by critical membrane damage of long alkyl chain and the subsequent leakage of intracellular constituents. The inflection point of "composite" compound **11** occurred at lower concentration, and the final uptake (9.2 μg/10^9cells) was higher than 6.4 μg/10^9cells of unchlorinated compound **8**. The cell wall of gram-positive MRSA consists of several peptidoglycan layers which are crosslinked by peptides, encircling the cell membrane. During the insertion of long alkyl chain into the thick peptidoglycan layer, *N*-chloramide within the same molecular structure of compound **11** might exert its oxidative effect on peptides, causing the breakage of the cross-linkers. It leads to a loosen cell wall and higher surface area for the uptake of more biocides. Ultimately, the cell

wall is disintegrated and more cytoplasmic constituents are exposed, which provide more binding sites. Overall, *N*-chloramide might be able to accelerate the disintegration of cell wall and facilitate the insertion of long alkyl chain into cytoplasmic membrane, resulting in a synergistic effect with the fastest killing kinetics of "composite" compound **11** against MRSA. The difference in uptake isotherms of tetradecyl **9** and **12** was much smaller, coincident with the time-kill profiles.

The uptake isotherms of compound **8** and **9** against MDR *P. aeruginosa* in Fig. 11 (B) obeyed L2 pattern, arriving at the final plateau with a maximum of 2.9 μg/10^9cells and 9.3 μg/10^9cells, respectively. The uptakes were generally lower than MRSA, owing to its rigid outer membrane which acted as a barrier to prevent the access of biocides. There appeared to be a limit in the amount of adsorption of long-chained QA salts alone, especially compound **8**. This observation could be linked to the killing kinetics where a plateau effect was observed, suggesting no further killing of cells. However, the uptake profiles of "composite" compound **11** and **12** after chlorination turned to follow L3 pattern, continuing to increase with the rising concentration to 8.8 μg/10^9 cells and 12.6 μg/10^9 cells, respectively.

Critical membrane damage of bacterial cells arising from the insertion of hydrophobic tails of long-chained QA salts, plays a decisive role in the rapid cell death. In gram-negative *P. aeruginosa*, there exist an outer membrane and a periplasmic space between the outer membrane and cytoplasmic membrane. The periplasma may constitute up to 40% of the total cell volume, which provide abundant proteins sites to attract the attack of *N*-chloramide of compound **4** to form a chlorine cover of 2.54×10^{-17} mol Cl^+/CFU. It does not impair the cell viability but it will protect the cytoplasmic membrane from the insertion of long alkyl chain of compound **8** or **9**, giving the slowest killing kinetics of the mixture of separate components. Similarly, the *N*-chloramide head of compound **11** and **12** also has a high affinity to proteins site in periplsama, leaving the long

alkyl chain facing outwards. The killing action of *N*-chloramide is much more sluggish via three steps, as compared to the direct physical damage of long chain (compound **8** and **9**), resulting in a slower increase in the absorption and thus killing efficacy in the beginning. After that, the uptake and bacterial reduction of "composite" compound **11** increased consistently while no further increase was noted for unchlorinated compound **8**. The stagnant absorption and bactericidal efficacy might prompt some speculations on the bacterial resistance towards QA salts, which can be facilitated by several mechanisms including intrinsic insusceptibility or impermeability, overexpression of efflux pumps and modification of lipopolysaccharide in the outer membrane of *P. aeruginosa*.[49] Since there existed a big difference in the uptake isotherms and antibacterial activity of biocides before and after chlorination (compound **8** and **11**), the overexpression of efflux pumps might be the reason for the possible resistance to long-chained QA salts.

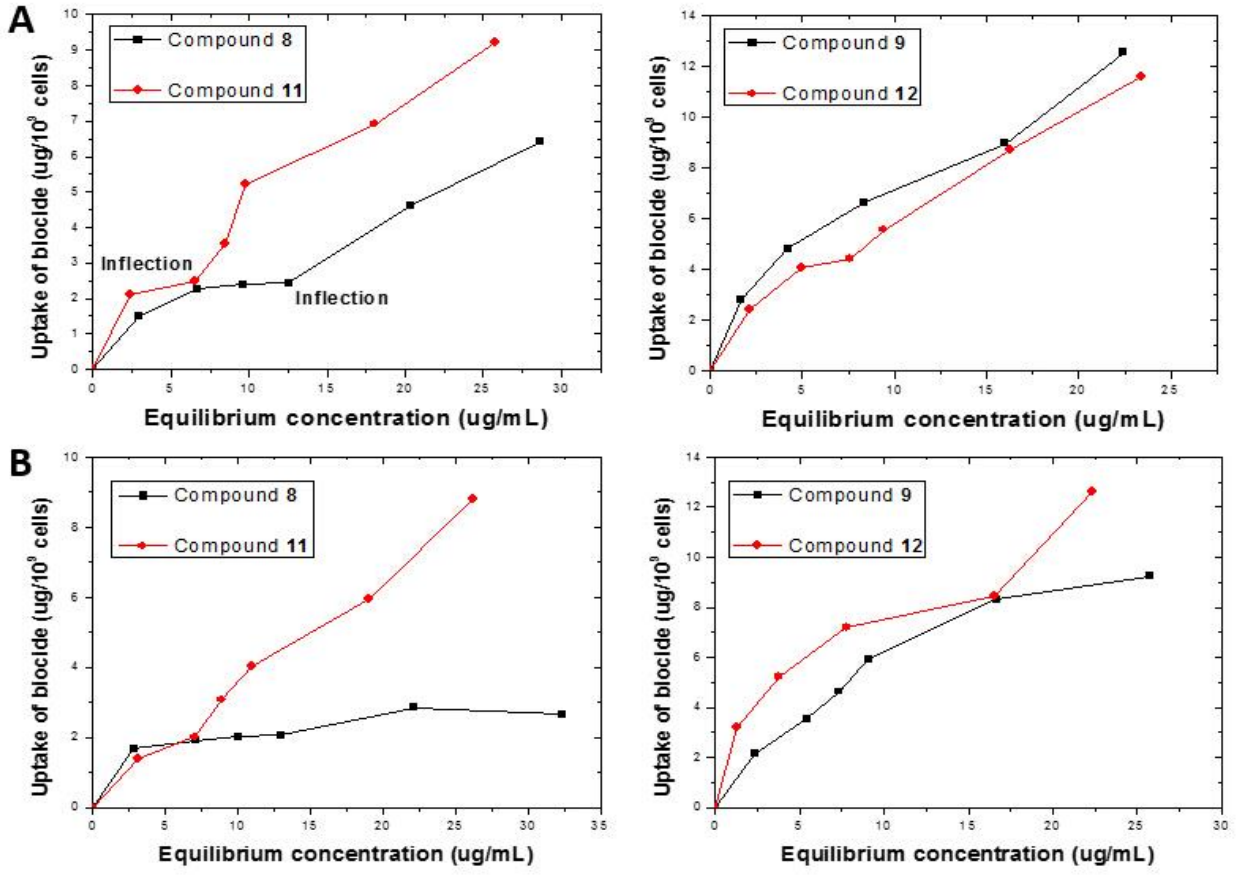

Fig. 11. Uptake isotherms of compound **8-12** against (A) 2.70×10^9 CFU/mL of MRSA and (B) 1.54×10^9 CFU/mL of MDR *P. aeruginosa* in PBS (0.1 M, pH 7.4).

Efflux pumps are proteinaceous transporters to pump out biocides from bacterial cells. Specifically, resistance-nodulation-division (RND) efflux pumps are one of the most important determinants of MDR in gram-negative bacteria, which pump out the biocides directly from the outer leaflet of the inner membrane bilayer.[139] Fernando and Kumar[139] have summarized the antibiotic substrates of RND pumps in *P. aeruginosa* as listed in Table 6. MDR *P. aeruginosa* (73104) used in this study was obtained from the University of Alberta Hospital, accompanied with the data of antibiotic resistance isolates (Table 7). Unfortunately, the designated antibiotic substrates in RND pumps were not included in Table 7. Therefore, we used five *P. aeruginosa* bacterial stains with different genotypes (Table 8) to identify the efflux pumps responsible for the resistance towards long-chained QA salts. The MICs of compound **8**, **9**, **11**, and **12** against each strain was listed in Fig. 12. No difference was detected in the MICs between PA 01 and PA 0200, excluding the possibility of ΔMexCD-OprM pump. However, there existed a decrease in the MIC against PA 0200 to PA 0238 in the absence of ΔMexCD-OprJ pump, and a further decrease from PA0238 to PA0386 without ΔMexJK, ΔMexXY, and opmH protein. ΔMexJK pump is generally silent, hence, ΔMexCD-OprJ and ΔMexXY pumps might be the potential ones involved in the resistance towards long-chained QA salts. Besides, opmH protein can work with other efflux pumps as well. After chlorination, *N*-chloramide of "composite" compound**s** is able to attack and disable the efflux pumps due to the oxidation of active chlorine to proteins, resulting in the consistent uptake and bactericidal efficiency. The introduction of *N*-chloramide into the structure of long-chained QA salts has great potential to serve as a possible way of overcoming the problem of bacterial resistance.

Table 6. Examples of resistance-nodulation-division (RND) pumps from gram-negative *P. aeruginosa* with their antibiotic substrates.[140]

Pump	Antibiotic substrates
MexAB-OprM	β-lactams, Chloramphenicol, Ethidium bromide, Fluroquinolones, Macrolides, Quinolones, Tetracycline,
MexCD-OprJ	β-lactams, Chloramphenicol, Fluroquinolones, Novobiocin, Tetracycline, Trimethoprim,
MexEF-OprN	Chloramphenicol, Fluroquinolones, Trimethoprim,
MexXY	Aminoglycoside, Macrolides, Tetracyclines,
MuxBC-OpmB	β-lactams, Macrolides Novobiocin, Tetracycline.

Table 7. Minimal inhibitory concentrations (MICs) of antibiotics against MDR *P. aeruginosa* (73104).

Antibiotic	MIC
Amikacin	>64
Cefazolin	>128
Ceftriaxone	256
Ciprofloxacin	>16
Clarithromycin	>16
Clindamycin	>8
Daptomycin	>32
Doripenem	>64
Gentamicin	>32

Levofloxacin	>32
Linezolid	>32
Meropenem	>64
Moxifloxacin	>16
Piperacillin Tazobactam	64
Tigecycline	>16
Trimethoprim Sulfa	>8
Vancomycin	>8

Table 8. *P. aeruginosa* stains with different genotypes for identification of efflux pumps.

Strain	**Genotype**
PA 01	Wild type
PA 0200	Absence of ΔMexCD-OprM
PA 0238	Absence of ΔMexCD-OprM, ΔMexCD-OprJ
PA 0386	Absence of ΔMexCD-OprM, ΔMexCD-OprJ, ΔMexJK, ΔMexXY, opmH
PA 01172	Absence of ΔMexCD-OprM, ΔMexCD-OprJ, ΔMexJK, ΔMexXY, ΔMexEF-OprN, ΔtriABC

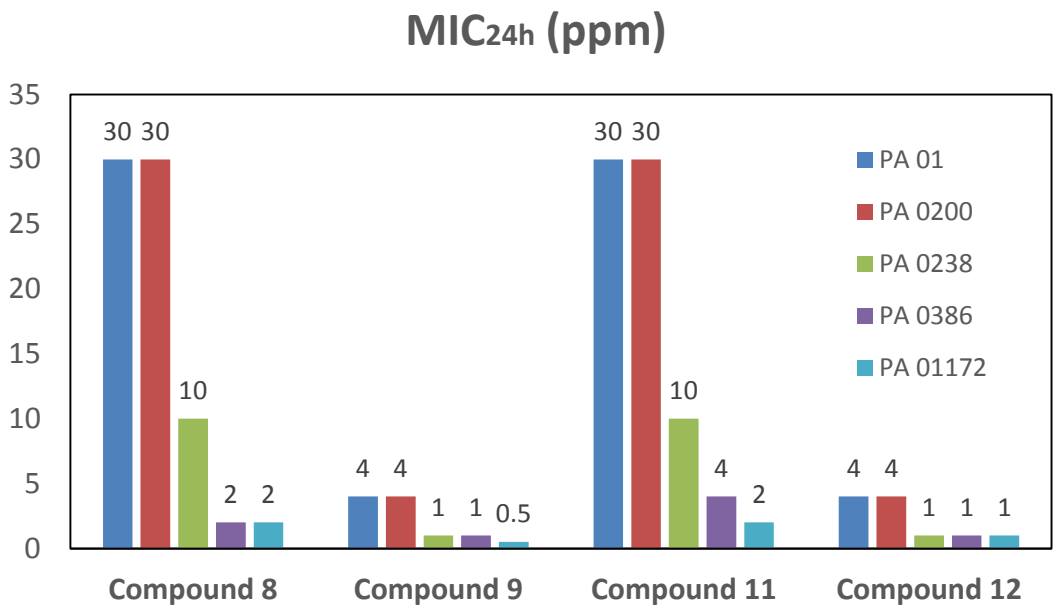

Fig. 12. Minimal inhibitory concentrations (MIC_{24h}) of compound **8**, **9**, **11**, and **12** against five *P. aeruginosa* stains with different genotypes.

4.3.2 MIC results.

On the basis of the static antibacterial results, compound **8-12** with long alkyl chain are selected to be incorporated into hydrogel dressings for drug delivery. Thus, the MICs and cytotoxicity were evaluated to obtain a referential drug releasing region to achieve adequate microbial killing but minimal cytotoxicity. By contrast, the MIC of short-chained compound **4** was also determined under the assay conditions used herein. It presented unsatisfactory toxicity against both MRSA and MDR *P. aeruginosa* with the MIC_{24h} dose of 256 ppm as shown in Table 9. Increasing the alkyl chain length from methyl **4** to dodecyl **11** and tetradecyl **12** resulted in a significant decrease in MIC_{24h} in broth from 256 ppm to 8 ppm and 1 ppm against MRSA and 32 and 8 ppm against MDR *P. aeruginosa*, respectively, suggesting a promoted killing efficiency. It is due to the

additional antibacterial action of long alkyl chain by inserting into cell membrane, causing physical damage. Generally, *P. aeruginosa* is less sensitive than MRSA owing to different chemical compositions of cell wall/membrane. The outer membrane of gram-negative bacteria exerts intrinsic resistance to the compound to access the cytoplasm. Different with the static antibacterial results, no significant difference in the MICs was noted between compound **8** and **11**, or compound **9** and **12**. The highly-efficient antibacterial activity of "composite" compound **11** or **12** mainly results from the long alkyl chain, hence, the MIC results are strongly dependent on the dose of long chain. The introduction of *N*-chloramide might be only reflected in the acceleration of the killing action, generating a faster killing kinetics than compound **8** and **9** in the static antibacterial test.

Table 9. Minimal inhibitory concentrations (MIC_{24h}) against MRSA and MDR *P. aeruginosa* and minimum cytotoxicity concentration (CT_{50}) against human fibroblast cells for compound **4, 8-12**.

Compounds	MRSA	MDR *P. aeruginosa*	CT_{50} against human fibroblast cells
	$MIC_{24\ h}$		
	ppm	ppm	ppm
4	256	256	57.44
8	8	32	2.47
9	1	8	0.65
11	8	32	3.6
12	1	8	0.68

4.3.3 *In vitro* cytotoxicity.

The cytotoxicity of compound **8-12** was evaluated against human dermal fibroblasts involved in the wound healing and immune responses. The viability of fibroblast cells was monitored via the MTT assay following 24 h exposure to different concentrations of each compound. Minimum cytotoxicity concentration (CT_{50}) is defined as the concentration that induced morphometric changes in 50% of the cells or 50% cell death. As seen from Table 9, compound **4** exhibited the CT_{50} of 57.44 ppm, much lower than the MIC_{24h} of 256 ppm. And longer alkyl chain in compound **8-12** led to a dramatic decrease in the CT_{50}, lower than the corresponding MIC_{24h}, especially against MDR *P. aeruginosa*. The results suggest that QA salts are relatively toxic to human fibroblast cells, which are consistent with previously reports that QA salts were mostly restricted in topical application due to their cytotoxicity, in spite of their therapeutic potential.[140-1] To alleviate the problem, there are emerging trends in the development of macromolecular antimicrobials with high selectivity, aiming to decrease the cytotoxicity while retaining the efficient antibacterial activity. Carpenter *et al.*[48] proved that the cytotoxicity against fibroblasts was notably less after tethering QA salts to silica nanoparticles. Engler *et al.*[142] also demonstrated that antimicrobial polycarbonates, incorporated with sufficient cationic charge and hydrophobic moiety, could selectively target and kill microbes without exerting toxicity on mammalian cells. Since "composite" compounds with *N*-chloramide and long alkyl chain exert an enhanced, even synergistic effect to fight multi-drug-resistant infections, future work in this study is to decrease their cytotoxicity via the synthesis of macromolecules comprising these dual functional structures.

4.4 The loading and release of biocides.

Although compound **8**, **9**, **11**, and **12** with long alkyl chain was highly toxic to human cells, the loading and release of these compounds into hydrogel deposited PET fabrics were still conducted

as the tentative experiment to provide some prospective results for future study. The use of hydrogels in drug delivery applications has presently sparked particular interest. The porosity of these three-dimensional, cross-linked networks allows drug loading and subsequent releasing at a rate which is dependent on the diffusion coefficient of the drugs through the gel matrix.[115-7] Additionally, hydrogels are highly biocompatible with living tissues due to the similar physiochemical properties of high water content, soft and rubbery consistency, and low interfacial tension with water or biological fluids.[143]

In this study, a post-loading method was used by keeping the initially dry, pre-formed PET-PAm samples in biocide solution (0.0282 M). The PAm hydrogel would swell in the solution and form a gel network, which allowed the diffusion of biocides. The weight increment of hydrogel samples and %loading of biocides are shown in Table 10. All the samples absorbed around 6.5% of biocide solution, which served as the volume change of loading solution to calculate the %loading (based on UV absorbance) before and after loading. The %loading of compound **8** arrived at 5.44%, higher than 3.57% of compound **9**. It might be attributed to the lower bulk of compound **8** which facilitated its diffusion into the hydrogel matrix. Unexpectedly, "composite" compound **11** and **12** showed a significant increase in the loading capacity. There is subtle, or even negligible difference in the solubility and dissolution of compound **11** or **12** and long-chained **8** or **9**, except for the substitution of *N*-H with *N*-Cl during the chlorination process. This finding prompted speculation on the interaction of *N*-chloramide (*N*-Cl) with PAm hydrogel, which might promote the uptake of chlorinated biocides into the hydrogel system.

A reversible transfer reaction for chlorine between chloramines and amines has been reported since the 20th century, which is named "transchlorination" as designated in Scheme 4. The occurrence of transchlorination will cause the dechlorination of compound **11** and **12** to their unchlorinated

counterparts (**8** and **9**), which cannot be detected by spectrophotometer. Therefore, a versatile method was used to determine the chlorine consumption after loading by direct titration with sodium thiosulfate ($Na_2S_2O_3$), while potassium iodide (KI) in conjunction with starch solution was used as an indicator. It was found that the chlorine consumption of compound **11** and **12** reached as high as 45.79% and 39.49%, respectively, as compared to the %loading** of 11.02% and 11.48% based on UV absorbance (Table 10). It suggests that the reaction of chlorine transfer from *N*-chloramide to the amine groups in PAm hydrogel do eventuate, that is to say, not only "composite" compounds (**11** and **12**) but also long-chained QA salts (**8** and **9**) resulted from transchlorination are responsible for the UV absorbance in the remaining loading solution. And the proportion of these two components can be calculated with combinations of the data of chlorine consumption and UV absorbance of A_0 (before loading) and A_1 (after loading). For example, there was 45.79% of chlorine consumption of compound **11** after loading, including the portion loaded into PET-PAm and the portion converted to compound **8**. It means (1-45.79%) of compound **11** was left over in the loading solution, contributing (1-45.79%) $\times A_0$ to the UV absorbance after loading (A_1). Hence, the contribution of compound **8** to UV absorbance was knowable as A_1 - (1-45.79%) $\times A_0$. Then the amount of residual compound **11** and dechlorinated compound **11** (converted to compound **8**) after loading could be calculated, and the amount of compound **11** loaded into PAm hydrogel was ultimately obtained via subtraction from the gross. As shown in Table 8, the converted portion of compound **11** and **12** (%transchlorination) occupied a proportion of 33.31% and 30.15%, respectively, as compared to 15.90% and 13.47% of the portion loaded into the hydrogel system (%loading***). It indicates the majority of the chlorine consumption of compound **11** and **12** during the loading process results from the reaction of transchlorination. Gottardi[144] mentioned that transchlorination was an essential property of *N*-chloro compounds to expound the

antibacterial activity. It is catalyst-free, reversible and thus comes to an equilibrium, while the oxidizing capacity of active chlorine is retained. Generally, apart from the diffusion and dissolution of biocides, the biocide-polymer interaction is considered as another major force for the uptake of biocides.

Table 10. The loading of biocides into PET-PAm hydrogel.

Sample	Weight increment (%)	%loading**	Chlorine consumption (%)	%transchlorination	%loading***
Compound **8**	6.60 ± 0.08	5.44 ± 0.50	N/A*	N/A	N/A
Compound **9**	6.75 ± 0.23	3.57 ± 0.30	N/A	N/A	N/A
Compound **11**	6.26 ± 0.33	11.02 ± 2.87	45.79 ± 7.40	33.31 ± 3.71	15.90 ± 2.91
Compound **12**	6.74 ± 0.36	11.48 ± 1.93	39.49 ± 1.61	30.15 ± 0.88	13.47 ± 1.93

*N/A means NOT applicable.

%loading was calculated based on the decrease in the UV absorbance after loading, assuming there was no transchlorination of compound **11 and **12**.

***%loading of compound **11** and 12 was calculated based on the combination of chlorine consumption and UV absorbance after loading, which was the realistic amount of these two biocides loaded into PAm hydrogel.

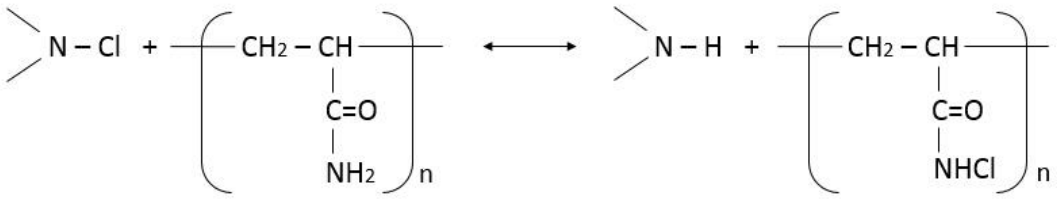

Scheme 4. Equation of transchlorination reaction between *N*-chloramide and polyacrylamide.

The importance of preventing infections has been well recognized to achieve successful burn care. Medicated dressings by incorporating germicidal compounds provide an inherent antibacterial activity through a consistent and sustained mechanism over long periods of time. The study of drug release kinetics contributes to maximize the efficiency in infection control depending on the condition of burn wounds. It is of crucial importance for immediate response to the presence of bacterial flora at the onset of an infection, to avoid the formation of biofilms which are notoriously difficult to eradicate.[145] Following the initial release, a consistent and sustained release of antimicrobials at an effective level is preventive against the occurrence of latent infection. Here, release kinetics of compound **8**, **9**, **11**, and **12** from PET-PAm samples (2×2 cm^2) were conducted in 10 mL of PBS (0.1 M, pH 7.4). Skin temperature 32 ℃ was selected for *in vitro* release studies to simulate the microenvironment of real wounds. At a desired time interval, an aliquot (500 μL) was removed and mixed with Orange II dye to form dye-salt complexes, which could be extracted by chloroform for quantification through UV measurement at 485 nm.

We previously stated that the reaction of chlorine transfer occurred from *N*-chloramide to PAm hydrogel, which boosted the loading efficiency of compound **11** and **12**. It might be possible the transchlorination continues for the loaded portion of compound **11** and **12** during the releasing process or during the preservation prior to the release studies. To verify it, the releasing medium (after 540 min of release) was titrated with $Na_2S_2O_3$ and only a tiny amount of compound **11** or **12** with active chlorine was detected, accounting for around 2% of loaded biocides. Thus, the dominant component in the releasing medium was unchlorinated compound **8** or **9** which arose from the unremitting transchlorination. 5% KI solution was added onto the surface of PET-PAm samples after the release of "composite" compound **11** and unchlorinated compound **8** for comparison. There was no color change of the sample of compound 8 (Left in Fig. 13). However,

the color of the sample of compound **11** (Right in Fig. 13) turned to intensive yellow, indicating the presence of substantial active chlorine on the surface of PET-PAm, where a redox reaction with KI took place and generated yellow I_2. The same applied to the sample of compound **12**. Overall, the results evince that "composite" biocides (**11** and **12**) functions as two separate components during the release from PAm hydrogel because of the transchlorination. The resultant counterpart (**8** or **9**) is consistently released in the release medium while oxidative chlorine is retained on the surface of PET-PAm dressing.

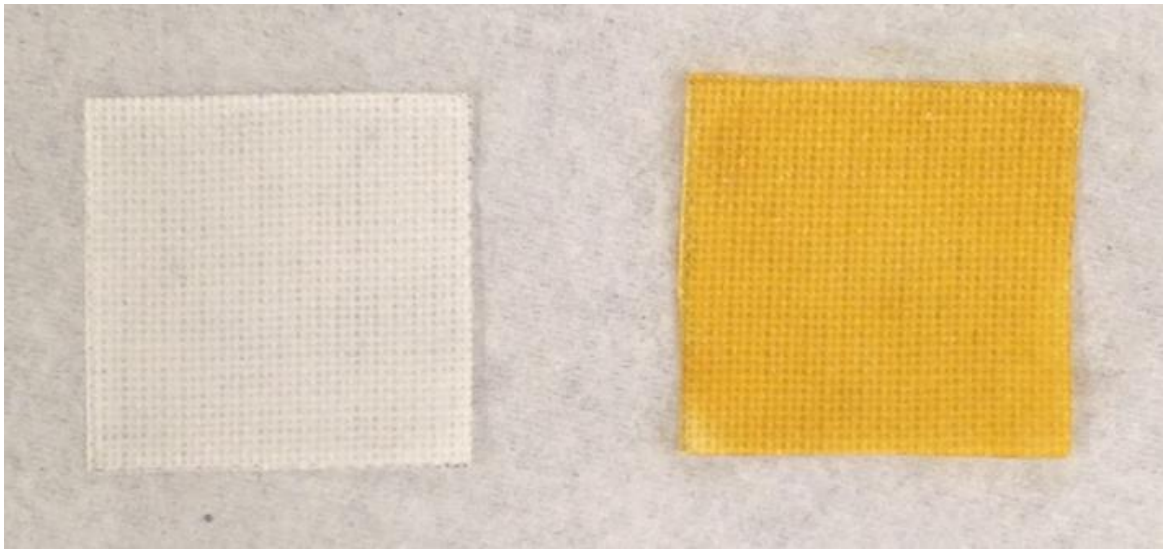

Fig. 13. KI treated PET-PAm samples after 540 min release of compound **8** (Left) and compound **11** (Right).

Fig. 14 shows the release profiles of compound **8-12** from PET-PAm samples within 540 min. The release of "composite" compounds (**11** and **12)** was calculated based on the UV absorbance using the standard calibration curve of their dechlorinated counterparts (**8** and **9**), which were proved to be the dominant components in the release medium due to the transchlorination. It was observed that all the biocides arrived at more than 90% of released within 9 hours. It came to an approximately full release of compound **8** and **9** within only 1 hour, which might be attributed to

their lower loading capacity. The percentage of burst release of compound **11** and **12** was lower as compared to that of compound **8** and **9**. It might be due to the slower swelling of chlorinated PAm hydrogel arising from the chlorine transfer reaction with compound **11** and **12**. After the burst release at the initial stage, there was a slower release of these two "composite" compounds because of the lessen concentration gradient.

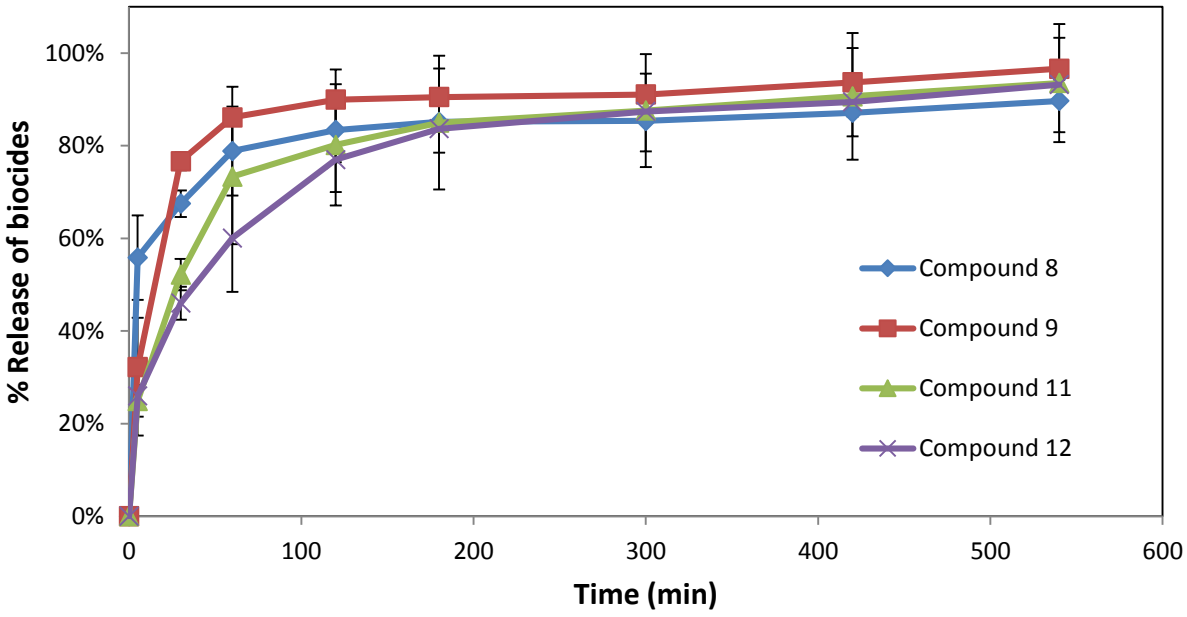

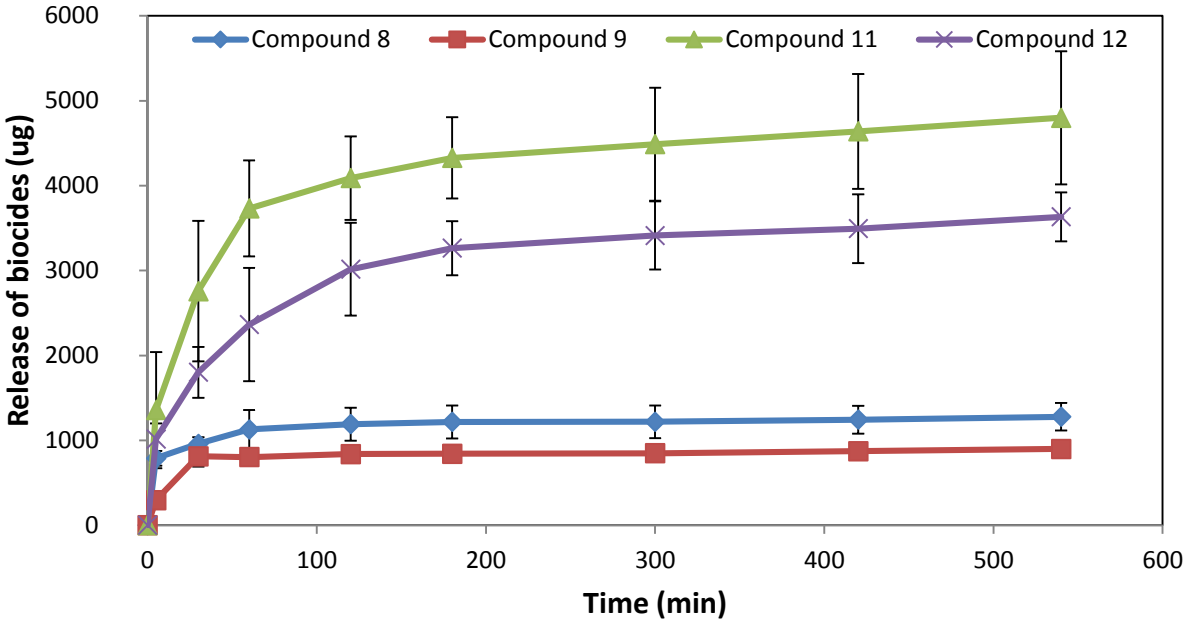

Fig. 14. Release of compound **8**, **9**, **11**, and **12** versus time curves of PET-PAm samples. The error bars represent standard deviation based on triplicate analysis.

The release of biocides from the dried, pre-loaded PET-PAm hydrogel samples involved the absorption of water into the matrix and simultaneous desorption of biocides via diffusion. The process could be modeled using a free-volume approach or a swelling-controlled release mechanism. A common equation was introduced to characterize the free-volume mechanism of drug diffusion in polymers: $(M_t/M_\infty) = kt^n$, where M_t/M_∞ is fraction of drug released during time t, k is kinetic constant incorporating structural and geometric characteristics of the delivery system, and n is diffusion exponent indicative of the type of drug transport phenomenon.[146] The values of k and n of compound **8**, **9**, **11** and **12** were calculated and the results were included in Table 11. The release exponent $n \leq 0.5$ for Fickian diffusion release from slab, $0.5 < n < 1.0$ for non-Fickian diffusion which means that drug release followed both diffusion and erosion controlled mechanism, and $n = 1$ for zero order release, where drug release is independent of time. The values of n

calculated for these four compounds were all lower than 0.5, indicating a Fickian transport.[118] Specifically, the lowest of diffusion exponent *n* (0.1322) of compound **8** was a result of the extremely high initial release of 55.86% within 5 min, which might not be suitable in the equation.

Table 11. Analysis of release kinetics of compound **8**, **9**, **11** and **12**.

Sample	Diffusion exponent, *n*	*k*	Correlation coefficient, *r*
Compound **8**	0.1322	0.4469	0.9813
Compound **9**	0.4135	0.1702	0.9864
Compound **11**	0.4312	0.1223	0.9992
Compound **12**	0.3095	0.1631	0.9999

We previously stated that the release of "composite" compounds actually functions as two separate components: long-chained QA moieties are consistently released to wound sites for inactivation of bacteria, while active chlorine with its oxidizing capacity is retained on the PET-PAm dressing to prevent further infection from exogenous sources in the environment. This type of wound dressing perfectly meets the expectations of clinicians and patients for the prevention and treatment of burn wound infections. However, it loses the advantages of covalently combining *N*-chloramide and QA moieties in the same molecular structure to enhance the bactericidal efficacy and simultaneously eliminate or reduce bacterial resistance. Therefore, the interaction between "composite" biocides with PAm hydrogel should be avoided. Other types of hydrogels, such as polyethylene glycol (PEG) based hydrogels can be deposited onto PET dressings in place of PAm hydrogel.[147] The loading capacity of biocides can be adjusted by manipulating the polymer composition and altering the cross-linking density. The efficiency of biocide delivery can be

further improved with the copolymerization with intelligent hydrogels which are able to change their dimensions in response of environmental changes such as temperature, pH and the presence of certain bacterial enzymes.[113, 148-9]

CHAPTER 5. CONCLUSIONS AND FUTURE STUDIES

Burn injuries are among the most devastating of all injuries and a major global public health crisis. It is necessary to develop an ideal burn wound dressing with a "wishing list" of properties required for burn care, of which non-adherence and antimicrobial activity are considered as the most important characteristics. First, an *in vitro* gelatin-based model is adapted to evaluate the adherence of current dressings by providing plentiful advantages over traditional bio-adhesion test or *in vivo* testing. According to the results of the peeling force test of PET fabrics, drying of fabric/gelatin complexes at 32 ^{o}C, 75% RH could better represent the optimal clinical situations. Water and surfactant solution do help ease the peeling of dressings from the gelatin model. The interfacial debonding between gelatin and PET can be achieved by applying 500 μL of water or surfactant onto the PET surface with an area of 16 × 60 mm^2, which affords practical guideline regarding how to effectively decrease the adherence of current commercially available wound dressings. Meanwhile, a thin layer of polyacrylamide (PAm) hydrogel grown from the surface of PET fabric also decreases the dressing adherence to a great extent, without significantly compromising its flexibility and conformability. This hydrogel layer has a great potential to serve as a reservoir for incorporating with active agents due to its unique physiochemical properties.

Novel "composite" biocides combining *N*-chloramide and short-chained QA moiety exert efficient antibacterial activity against both MRSA and MDR *P. aeruginosa*, as compared to short-chained QA salts alone. There is no significant difference among "composite" compound **4-6** with different ratios of QA moiety/*N*-chloramide against MRSA, while compound **5** with lowest ratio exerts the slowest killing kinetics against MDR *P. aeruginosa*. No synergistic, but antagonistic effect is noted in "composite" compound **10** after increasing the alkyl chain length to hexyl group. Further increasing the alkyl chain length of QA moiety to dodecyl and tetradecyl group results in a boost

in the bactericidal efficacy, in virtue of the highly-efficient killing action by insertion of the long chain into cytoplasmic membrane. More important, the combination of *N*-chloramide and long-chained QA moiety demonstrates a synergistic effect against MRSA. *N*-chloramide exerts a great oxidative stress to peptides which cross-link multiple peptidoglycan layers encircling MRSA cells, which facilitates the disintegration of cell wall and thus the insertion of long alkyl chain into critical membrane. However, the accretion of *N*-chloramide tends to slow down the killing of long-chained QA salts alone against MDR *P. aeruginosa* at the beginning by competing for the binding affinity. A plateau is observed in the disinfection kinetics of long-chained QA salts, which might be attributed to the presence of RND efflux pumps. Covalently bonded *N*-chloramide could help overcome the problem, providing a sustainably efficient antibacterial activity. Overall, these "composite" compounds with long alkyl chain show their valuable therapeutic potentials with excellent bactericidal efficacy, but the high cytotoxicity limits their use in topical application. Top priority of future work is to decrease their toxicity to mammalian cells. Evidence is accumulating that macromolecular antimicrobials are the emerging trend in wound treatment, exerting satisfying bactericidal efficacy but low cytotoxicity. Thus, tethering these "composite" biocides to particles or polymers might be a feasible solution.

Finally, four compounds with long alkyl chain are selected for the *in vitro* release studies from PET-PAm dressings. The transchlorination from *N*-chloramide of "composite" compounds to PAm hydrogel motivates the uptake of biocides, resulting in a higher loading content. All the compounds arrived at more than 90% of biocide released from PAm hydrogel within 540 min, to achieve a both non-adherent and antibacterial wound dressings. However, the main component of "composite" biocide released in the dissolution medium is the unchlorinated counterpart, while the active chlorine is immobilized on the surface of PET-PAm. Thus, it is imperative to replace PAm

hydrogel with other types of hydrogels in future studies, to avoid the chlorine transfer. A possible group of candidates are polyethylene glycol (PEG) based hydrogels, where the biocide loading content can be controlled by manipulating the polymer composition. The introduction of thermo-responsive or pH-responsive hydrogels can further improve the biocide delivery efficiency.

REFERENCES

1. **Atiyeh BS, Gunn SW, Hayek SN.** 2005. State of the art in burn treatment. World J Surg. **29(2):**131-48.
2. **Sen S, Greenhalgh D, Palmieri T.** 2009. Review of burn injury research for the year 2009. J Burn Care Res. **31(6):**836-48.
3. **Jeschke MG, Herndon DN.** 2013. Burns in children: standard and new treatment. The Lancet. Available online: http://dx.doi.org/10.1016/S0140-6736(13)61093-4.
4. **Peck MD.** 2011. Epidemiology of burns throughout the world. Part I: Distribution and risk factors. Burns **37:**1087-100.
5. **Forjuoh SN.** 2006. Burns in low- and middle-income countries: A review of available literature on descriptive epidemiology, risk factors, treatment, and prevention. Burns **32:**529-37.
6. **Geneva, World Health Organization.** 2008. The global burden of disease: 2004 update. Available online: http://www.who.int/healthinfo/global_burden_disease/GBD_report_2004update_full.pdf.
7. **Rayner R, Prentice J.** 2011. Paediatric burns: A brief global review. Wound Practice & Research **19(1):**39-46.
8. **Duke J, Wood F, Semmens J, Edgar DW, Spilsbury K, Hendrie D, Rea S.** 2011. A study of burn hospitalizations for children younger than 5 years of age: 1983-2008. Pediatrics **127(4):**971-7.
9. **Cagle KM, Davis JW, Dominic W, Ebright S, Gonzales W.** 2006. Developing a focused scald-prevention program. J Burn Care Res. **27:**325-9.
10. **Burd A, Yueh C.** 2005. A global study of hospitalized paediatric burn patients. Burns **31:**432-8.
11. **Poulos RG, Hayen A, Chong SSS, Finch CF.** 2009. Geographic mapping as a tool for identifying communities at high risk of fire and burn injuries in children. Burns **35:**417-24.
12. **Spinks A, Wasiak J, Cleland H, Beben N, Macpherson AK.** 2008. Ten-year epidemiological study of pediatric burns in Canada. J Burn Care Res. **29(3):**482-8.
13. **Hermans MHE.** 2005. A general overview of burn care. International Wound Journal **2(3):**206-20.

14. **Sterling JP, Heimbach DM, Gibran NS.** 2010. 15 Management of the burn wound. Published online: DOI 10.2310/7800.S07C15.
15. **Kowalske KJ.** 2011. Burn wound care. Phys Med Rehabil Clin N Am. **22:**213-27.
16. **Wasiak J, Cleland H, Campbell F.** 2008. Dressings for superficial and partial thickness burns. Cochrane Databases Syst Rev. **4:**CD002106.
17. **Hettiaratchy S, Papini R.** 2004. Initial management of a major burn: II–assessment and resuscitation. BMJ **329:**101-3.
18. **Jones VJ.** 2006. The use of gauze: will it ever change? Int Wound J. **3:**79-86.
19. **Seaman S.** 2002. Dressing selection in chronic wound management. Journal of the American Podiatric Medical Association **92(1):**24-33.
20. **Selig HF, Lumenta DB, Giretzlehner M, Jeschke MG, Upton D, Kamolz LP.** 2012. The properties of an "ideal" burn wound dressing – What do we need in daily clinical practice? Results of a worldwide online survey among burn care specialists. Burns **38:**960-6.
21. **Sharma BR.** 2007. Infection in patients with severe burns: causes and prevention thereof. Infect Dis Clin N Am **21:**745-59.
22. **Macedo JLS, Santos JB.** 2005. Bacterial and fungal colonization of burn wounds. *Mem Inst Oswalso Cruz*, Rio de Janeiro **100(5):**535-9.
23. **Macedo JLS, Rosa SC, Castro C.** 2003. Sepsis in burned patients. Res Bras Med Trop. **36:**647-52.
24. **Vindenes H, Bjerknes R.** 1995. Microbial colonization of large wounds. Burns **21:**575-9.
25. **Lawrence JC.** 1992. Burn bacteriology during the last 50 years. Burns **18:**S23-29
26. **Agnihotri N, Gupta V, Joshi RM.** 2004. Aerobic bacterial isolates from burn wound infections and their antibiograms: a five-year study. Burns **30:**241-3.
27. **Church D, Elsayed S, Reid O, Winston B, Lindsay R.** 2006. Burn wound infections. Clin. Microbiol. Rev. **19(2):**403-34.
28. **Weber J, McManus A.** 2004. Infection control in burn patients. Burns **30:**A16-24.
29. **Mayer DA, Tsapogas MJ.** 1993. Povidone-iodine and wound healing: a critical review. Wounds **5:**14-23.
30. **Burks RI.** 1998. Povidone-iodine solution in wound treatment. Phys Ther. **78:**21-8.
31. **Morgan DA.** 1999. Wound management products in the drug tariff. Pharm J. **263:**820-5.
32. **Boateng JS, Matthews KH, Stevens HNE, Eccleston GM.** 2008. Wound healing dressings

and drug delivery systems: A review. J Pharm Sci. **97(8):**2892-923.

33. **Lee JW, Park RJH.** 2000. Bioadhesive-based dosage forms: The next generation. J Pharm Sci. **89:**850-66.
34. **Ummadi S, Shravani B, Rao NGR, Reddy MS, Nayak BS.** 2013. Overview on controlled release dosage form. **3(4):**258-69.
35. **Dusane AR, Gaikward PD, Bankar VH, Pawar SP.** 2011. A review on: sustained released technology. IJRAP **2(6):**1701-8.
36. **Uhrich KE.** 1999. Polymeric systems for controlled drug release. Chem Rev. **99:**3181-98.
37. **Alanis AJ.** 2005. Resistance to antibiotics: are we in the post-antibiotic era? Archives of Medical Research **36:**697-705.
38. **Golkar Z, Bagasra O, Pace DG.** 2014. Bacteriophage therapy: a potential solution for the antibiotic resistance crisis. J Infect Dev Ctries **8(2):**129-36.
39. **Lipsky BA, Hoey C.** 2009. Topical antimicrobial therapy for treating chronic wounds. Clinical Practice **49:**1541-9.
40. **Cookson BD, Farrelly H, Stapleton P, Gravey RPJ, Price MR.** 1991. Transferable resistance to triclosan in MRSA. Lancet **337(8756):**1548-9.
41. **Suller MT, Russel AD.** 2000. Triclosan and antibiotic resistance in *Staphylococcus aureus*. J Antimicrob Chemother **46(1):**11-8.
42. **Chuanchen R, Beinlick K, Hoang TT, Becher A, Karkoof-Schweizer RR, Schweizer HP.** 2001. Cross-resistance between triclosan and antibiotics in *Pseudomonas aeruginosa* is mediated by multidrug efflux pumps: exposure of a susceptible mutant strain to triclosan selescts *nfxB* mutants overexpressing MexCD-OprJ. Antimicrob. Agents Chemother. **45:**428-32.
43. **Tischer M, Pradel G, Ohlsen K, Holzgrabe U.** 2012. Quaternary ammonium salts and their antimicrobial potential: targets or nonspecific interactions? ChemMedChem **7:**22-31.
44. **Jiang S, Wang L, Yu H, Chen Y.** 2005. Preparation of crosslinked polystyrenes with quaternary ammonium and their antibacterial behavior. React Funct Polym. **62(2):**209-13.
45. **Yao C, Li X, Neoh KG, Shi Z, Kang ET.** 2008. Surface modification and antibacterial activity of electrospun polyurethane fibrous membranes with quaternary ammonium moieties. J Membr Sci. **320:**259-67.
46. **Li F, Weir MD, Xu HH.** 2013. Effects of quaternary ammonium chain length on antibacterial

bonding agents. J Dent Res. **92(10):**932-8.

47. **Simoncic B, Tomsic B.** 2010. Structures of novel antimicrobial agents for textiles – A review. Text Res J. **80:**1721-37.
48. **Carpenter AW, Worley BV, Slomberg DL, Schoenfisch MH.** 2012. Dual action antimicrobials: nitric oxide release from quaternary ammonium-functionalized silica nanoparticles. Biomacromolecules **13(10):**3334-42.
49. **Hegstad K, Langsrud S, Lunestad BT, Scheie AA, Sunde M, Yazadankhah SP.** 2010. Does the wide use of quaternary ammonium compounds enhance the selection and spread of antimicrobial resistance and thus threaten our health? Microbial drug resistance **16(2):**91-104.
50. **Bragg R, Jansen A, Coetzee M, van der Westhuizen W, Boucher.** 2014. Bacterial resistance to Quaternary Ammonium Compounds (QAC) disinfectants. Adv Exp Med Biol. **808:**1-13.
51. **Sundheim G, Langsrud S, Heir E, Holck AL.** 1998. Bacterial resistance to disinfectants containing quaternary ammonium compounds. Hygiene and Disinfection **41(3-4):**235-9.
52. **Meyer B, Cookson B.** 2010. Does microbial resistance or adaptation to biocides create a hazard in infection prevention and control? Journal of Hospital Infection **76:**200-5.
53. **Dai T, Huang YY, Sharma SK, Hashmi JT, Kurup DB, Hamblin MR.** 2010. Topical antimicrobials for burn wound infections. Recent Pat Antiinfect Drug Discov. **5(2):**124-51.
54. **Margaret LP, Lui SL, Poon VKM, Lung I, Burd A.** 2006. Antimicrobial activities of silver dressings: an *in vitro* comparison. Journal of Medical Microbiology **55:**59-63.
55. **Fong J, Wood F.** 2006. Nanocrystalline silver dressings in wound management: a review. International Journal of Nanomedicine **1(4):**441-9.
56. **Khundkar R, Malic C, Burge T.** 2010. Use of ActicoatTM dressings in burns: What is the evidence? Burns **36:**751-8.
57. **Dowsett C.** 2003. An overview of Acticoat dressing in wound management. British Journal of Nursing **12(9):**S44-9.
58. **Rustogi R, Mill J, Fraser JF, Kimble RM.** 2005. The use of Acticoat^{TM} in neonatal burns. Burns 31:878-82.
59. **Chlopra I.** 2007. The increasing use of silver-based products as antimicrobial agents: a useful development or a cause for concern? Journal of Antimicrobial Chemotherapy **59:**587-90.
60. **Silver S, Phung LT, Silver G.** 2006. Silver as biocides in burn and wound dressings and

bacterial resistance to silver compounds. Journal of Industrial Microbiology and Biotechnology **33(7):**627-34.

61. **Worley SD, Williams DE, Crawford RA.** 1988. Halamine water disinfectants. Crit Rev Env Contr. **18(2):**133-75.
62. **Barnela SB, Worley SD, Williams DE.** 2006. Syntheses and antibacterial activity of new *N*-halamine compounds. J Pharmm Sci. **76(3):**245-7.
63. **Liang J, Wu R, Wang JW, Barnes K, Worley SD, Cho U, Lee J, Broughton RM, Huang TS.** 2007. *N*-halamine biocidal coatings. J Ind Microbiol Biotechnol **34:**157-63.
64. **Hui F, Debiemme-Chouvy C.** 2013. Antimicrobial *N*-halamine polymers and coatings: A review of their synthesis, characterization, and applications. Biomacromolecules **14:**585-601.
65. **Chen Z, Sun Y.** 2006. *N*-halamine-based antimicrobial additives for polymers: preparation, characterization, and antimicrobial activity. Ind Eng Chem Res. **45:**2634-40.
66. **Gottardi W, Debabov D, Nagl M.** 2013. *N*-chloramines, a promising class of well-tolerated topical anti-infective. Antimicrob Agents Chemother. **57(3):**1107-14.
67. **Li L, Pu T, Zhanel G, Zhao N, Ens W, Liu S.** 2012. New biocide with both N-Chloramine and quaternary ammonium salt moieties exerts enhanced bactericidal activity. Advanced Healthcare Materials **1(5):**609-20.
68. **Benbow M.** 2010. Managing wound pain: is there an "ideal" dressing? British Journal of Nursing **19(20):**1273-4.
69. **Bell C, McCarthy G.** 2010. The assessment and treatment of wound pain at dressing change. British Journal of Nursing **19(11):**S4-10.
70. **Rippon M, Davies P, White R**. 2012. Taking the trauma out of wound care: the importance of undisturbed healing. Journal of Wound Care **21(8):**359-68.
71. **Judkins K, Clark L.** 2010. Managing the pain of burn wounds. Wounds UK **6(1):**110-8.
72. **Byers JF, Bridges S, Kijek J, LaBorde P.** 2001. Burn patients' pain and anxiety experiences. J Burn Care Rehabil **22(2):**144-9.
73. **Browne AL, Andrews R, Schug SA, Wood F.** 2011. Persistent pain outcomes and patient satisfaction with pain management after burn injury. Clin J Pain **27(2):**136-44.
74. **Patterson DR, Tininenko J, Ptacek JT.** 2006. Pain during burn hospitalization predicts long-term outcome. J Burn Care Research **27(5):** 719-26.
75. **Woo KY.** 2010. Wound-related pain: anxiety, stress and wound healing. Wounds UK **6(4):**92-

8.

76. **Thomas S.** 2003. Atraumatic dressings. Available online: http://www.worldwidewounds.com/2003/january/Thomas/Atraumatic-Dressings.html
77. **White R.** 2005. Evidence for atraumatic soft silicone wound dressing use. Wounds UK **1(3):**104-9.
78. **Thomas S.** 2000. Alginate dressings in surgery and wound management – part 1. Journal of Wound Care **9(2):**56-60.
79. **Qin Y.** 2005. The characterization of alginate wound dressings with different fiber and textile structures. Journal of Applied Polymer Science **100:**2516-20.
80. **Rosdy M, Clauss LC.** 1990. Cytotoxicity testing of wound dressings using normal human keratinocytes in culture. J Biomed Mater Res. **24:**363-77.
81. **Suzuki Y, Nishimura Y, Tanihara M, Suzuki K, Nakamura T, Shimizu Y, Yamawaki Y, Kakimaru Y.** 1998. Evaluation of a novel alginate gel dressing: Cytotoxicity to fibroblasts *in vitro* and foreign-body reaction in pig skin *in vivo*. J Biomed Mater Res. **39:**317-22.
82. **Suzuki Y, Tanihara M, Nishimura Y, Suzuki K, Yamawaki Y, Kudo H, Kakimaru Y, Shimizu Y.** 1999. *In vivo* evaluation of a novel alginate dressing. J Biomed Mater Res. **48:**522-7.
83. **Thomas S.** 2008. Hydrocolloid dressings in the management of acute wounds: a review of the literature. International Wound Journal **5(5):**602-13.
84. **Morgan N.** 2013. What you need to know about hydrocolloid dressings. Wound Care Advisor **2(3):**28-30.
85. **Finnie A.** 2002. Hydrocolloids in wound management: pros and cons. British Journal of Community Nursing **7(7):**338-44.
86. **Walker M, Hobot JA, Newman GR, Bowler PG.** 2003. Scanning electron microscopic examination of bacterial immobilisation in a carboxtmethyl cellulose (AQUACEL®) and alginate dressings. Biomaterials **24:**883-90.
87. **Trudgian J.** 2000. Investigating the use of Aquaform Hydrogel in wound management. British Journal of Nursing **9(14):**943-8.
88. **Edwards J.** 2010. Hydrogels and their potential uses in burn wound management. British Journal of Nursing **19(11):**S12-6.
89. **Morris C.** 2006. Wound management and dressing selection. Wound Essentials **1:**178-83.

90. **Morgan N.** 2013. What you need to know about hydrogel dressings. Wound Care Advisor **2(6):**21-3.
91. **Beldon P.** 2010. How choose the appropriate dressing for each wound type. Wound Essentials **5:**140-4.
92. **UK Essays.** Hydrogels for wound healing applications. Available online: http://www.ukessays.com/dissertations/sciences/hydrogels.php
93. **White R, Morris C.** 2009. Mepitel: a non-adherent wound dressing with Safetac technology. British Journal of Nursing **18(1):**58-64.
94. **Fowler A.** 2006. Atraumatic dressings for non-complex burns. Practice Nursing **17(4):**193-6.
95. **Barrett S.** 2009. Mepilex® Ag: an antimicrobial, absorbent foam dressing with Safetac® technology. British Journal of Nursing **18(20):**S28-36.
96. **Walker M, Jones S, Parsons D, Booth R, Cochrane C, Bowler P.** 2011. Evaluation of low-adherent antimicrobial dressings. Wounds UK **7(3):**32-45.
97. **Matsumura H, Ahmatjan N, Ida Y, Imai R, Wanatabe K.** 2012. A model for quantitative evaluation of skin damage at adhesive wound dressing removal. Int Wound J. **10(3):**291-4.
98. **Waring M, Bielfeldt S, Matzold K, Wilhelm KP.** 2012. A new methodology for evaluating the damage to the skin barrier caused by repeated application and removal of adhesive dressings. Skin Research and Technology **0:**1-9.
99. **Shakespeare P.** 2001. Burn wound healing and skin substitutes. Burns **27:**517-22.
100. **Cochrane C, Rippon MG, Rogers A, Walmsley R, Knottenbelt D, Bowler P.** 1999. Application of an in vitro model to evaluate bioadhesion of fibroblasts and epithelial cells to two different dressings. Biomaterials **20:**1237-44.
101. **Rogers AA, Walmsley RS, Rippon MG, Bowler PG.** 1999. Adsorption of serum-derived proteins by primary dressings: implications for dressing adhesion to wounds. Journal of Wound Care **8(8):**403-6.
102. **Dong C, Mead E, Skalak R, Fung YC, Debes JC, Zapata-Sirvent RL, Andree C, Greenleaf G, Cooper M, Hansbrough JF.** 1993. Development of a device for measuring adherence of skin grafts to the wound surface. Annals of Biomedical Engineering **21:**51-5.
103. **Andrews EH, Kamyab I.** 1986. Adhesion of surgical dressings to wounds. A new *in vitro* model. Clinical Materials **1:**9-21.
104. **Rao KVR, Devi PK.** 1988. Swelling controlled-release systems: Recent developments and

applications. Int J Pharm. **48:**1-13.

105. **Bourke SL, Al-Kahalili M, Briggs T, Michniak BB, Kohn J, Poole-Warren LA.** 2003. A photo-crosslinked poly(vinyl alcohol) hydrogel growth factor release vehicle for wound healing applications. AAPS PharmSci. **5(4):**1-11.
106. **Luo Y, Kirke KR, Prestwich GD.** 2000. Cross-linked hyaluronic acid hydrogel films: New biomaterials for drug delivery. J Control Release **69:**169-84.
107. **Aoyagi S, Onishi H, Machida Y.** 2007. Novel chitosan wound dressing loaded with minocycline for the treatment of severe burn wounds. Int J Pharm **330:**138-45.
108. **Maeda M, Kadota K, Kajihara M, Sano A, Fujioka K.** 2001. Sustained release of human growth hormone (hGH) from collagen film and evaluation of effect on wound healing in mice. J Control Release **77:**261-72.
109. **Sawada Y, Ara M, Yotsuyanagi T, Sone K.** 1990. Treatment of dermal depth burn wounds with an antimicrobial agent-releasing silicone gel sheet. Burns **16:**347-52.
110. **Sawada Y, Tadashi O, Masazumi K, Kazunobu S, Koichi O, Sasaki J.** 1994. An evaluation of a new lactic acid polymer drug delivery system: A preliminary report. Br J Plast Surg. **47:**158-61.
111. **Sakchai W, Churrerat P, Srisagul S.** 2006. Development and in vitro evaluation of chitosan-eudra-git RS 30D composite wound dressings. AAPS Pharm SciTech. **7:**E1-6.
112. **Mangala E, Kumar TS, Baskar S, Rao KP.** 2003. Dev of chitosan/polyvinylalcohol blend membranes as burn dressings. Trends Biomater Artif Organs. **17:**34-40.
113. **Martin del Valle EM, Galan MA, Carbonell RG.** 2009. Drug delivery technologies: the way forward in the new decade. Ind. Eng. Chem. Res. **48:** 2475-86.
114. **Zarzycki R, Modrzejewska Z, Nawrotek K.** 2010. Drug release from hydrogel matrices. Ecological Chemistry and Enginieering **17(2):** 118-36.
115. **Kim SW, Bae YH, Okano T.** 1992. Hydrogels: swelling, drug loading, and release. Pharmaceutical Research **9(3):**283-90.
116. **Ganji F, Vesheghani-Farahani E.** 2009. Hydrogels in controlled drug delivery systems. Iranian Polymer Journal **18(1):**63-88.
117. **Hoffman AS.** 2002. Hydrogels for biomedical application. Advanced Drug Delivery Reviews **54:**3-12.
118. **Reddy TT, Kano A, Maruyama A, Hadano M, Takahara A.** 2008. Thermosensitive

transparent semi-interpenetrating polymer networks for wound dressing and cell adhesion control. Biomacromolecules **9:**1313-21.

119. **ASTM standard D 1388**. 1996. Standard test method for stiffness of fabrics. ASTM International, West Conshohocken, PA.
120. **Zhanel GG, Rossnagel E, Nichol K, Cox L, Karlowsky JA, Zelenitsky S, Noreddin AM, Hoban DJ.** 2011. Ceftaroline pharmacodynamics activity versus community-associated and healthcare-associated methicillin-resistant *Staphylococcus aureus*, heteroresistant vancomycin—ntermediate *S. aureus*, vancomycin-intermediate *S. aureus* and vancomtcin-resistant *S. aureus* using an in vitro model. J Antimicrob Chemother. **66:**1301-5.
121. **Ioannou CJ, Hanlon GW, Denyer SP.** 2007. Action of disinfectant quaternary ammonium compounds against *Staphylococcus aureus*. Antimicrob. Agents Chemother. **51(1):**296-306.
122. **Kaufman T, Alexander JW, Nathan P, Brackett KA, Macmillan BG.** 1983. The microclimate chamber: the effect of continuous topical administration of 96% oxygen and 75% relative humidity on the healing rate of experimental deep burns. J. Trauma **23(9):**806-15.
123. **Thomas S.** 1982. Wound dressing materials-testing and control. Pharm. J. **228:**576.
124. **Zhang C, Wang J, Fridley KJ.** 2012. Environmental-Assisted Subcritical Debonding of Epoxy-Concrete Interface. Journal of Composition for Construction **16(5):**563-71.
125. **Larmour CJ, Mccabe JF, Grodon PH.** 1998. An Ex *vivo* Investigation into the Effects of Chemical Solvents on the Debond Behaviour of Ceramic Orthodontic Brackets. British Journal of Orthodontics **25:**35-9.
126. **Pekala RW.** 1989. Low density, resorcinol-formaldehyde aerogels. 1989. US Patent No. 4873218.
127. **Bishop SM, Walker M, Rogers AA, Chen WYJ.** 2003. Importance of moisture balance at the wound-dressing interface. Journal of Wound Care **12(4):**125-8.
128. **Waring M, Butcher M.** 2011. An investigation into the conformability of wound dressings. Wounds $_{UK}$ **7(3):**14-24.
129. **Cumbers DC.** 1977. Bonding of Structures. US Patent No. 4035219.
130. **Megan S.** Superabsorbent Hydrogels: A study of the Most Effective Application of Cross-linked Polyacrylamide Polymers. Available online: http://www.amnh.org/learn-teach/young-naturalist-awards/winning-essays2/2009-winning-essays/superabsorbant-hydrogels-a-study-of-the-most-effective-application-of-cross-linked-polyacrylamide-polymers

131. **Bjarnsholt T, Kirketerp-Moller K, Jensen PO, Madsen KG, Phipps R, Krogfelt K, Hoiby N, Givskov M.** 2008. Why chronic wounds will not heal: a novel hypothesis. Wound Repair and Regen. **16(1):**2-10.
132. **Gottardi W, Nagl M.** 2005. Chlorine covers on living bacteria: the initial step in antimicrobial action of active chlorine compounds. Journal of Antimicrobial Chemotherapy **55:**475-82.
133. **Williams DE, Elder ED, Worley SD.** 1998. Is free halogen necessary for disinfection? Appl. Environ. Microbiol. **54(10):**2583-5.
134. **Denyer SP, Stewart GSAB.** 1998. Mechanism of action of disinfectants. Int. Biodeter. Biodegr. **41:**261-8.
135. **Nikaido H.** 1979. Permeability of the outer membrane of bacteria. Angew. Chem. Int. Ed. Engl. **18:**337-50.
136. **Rotem S, Radzishevsky IS, Bourdetsky D, Navon-Venezia S, Carmeli Y, Mor A.** 2008. Analogous oligo-acyl-lysines with distinct antibacterial mechanisms. FASEB J. **22(8):**2652-61.
137. **Chen CZ, Beck-Tan NC, Dhurjati P, van Dyk TK, LaRossa RA, Cooper SL.** 2000. Quaternary ammonium functionalized poly(propylene imine) dendrimers as effective antimicrobials: structure-activity studies. Biomacromolecules **1(3):**473-80.
138. **Giles CH, Smith D, Huitson A.** 1974. A general treatment and classification of the solute adsorption isotherm. I. Theoretical. J. Colloid Interface Sci. **47:**755-65.
139. **Fernando DM, Kumar A.** 2013. Resistance-Nodulation-Division multidrug efflux pump in Gram-negative bacteria: role in virulence. Antibiotics **2:**163-81.
140. **Thorsteinsson T, Masson M, Kristinsson KG, Hjalmarsdottir MA, Hilmarsson H, Loftsson T.** 2003. Soft antimicrobial agents: synthesis and activity of labile environmentally friendly long chain quaternary ammonium compounds. J. Med. Chem. **46(19):**4173-81.
141. **Lv HT, Zhang SB, Wang B, Cui SH, Yan J.** 2006. Toxicity of cationic lipids and cationic polymers in gene delivery. J. Controlled release **114(1):**100-9.
142. **Engler AC, Tan JPK, Ong ZY, Coady DJ, Ng VWL, Yang YY, Hedrick JL.** 2013. Antimicrobial polycarbonates: investigating the impact of balancing charge and hydrophobicity using a same-centered polymer approach. Biomacromolecules **14(12):**4331-9.
143. **Satish CS, Satish KP, Shivakumar HG.** 2006. Hydrogels as controlled drug delivery system:

synthesis, crosslinking, water and drug transport mechanism. Indian Journal of Pharmaceutical Sciences **68(2):**133-40.

144. **Gottardi W, Nagl M.** 2010. N-chlorotaurine, a natural antiseptic with outstanding tolerability. J. Antimicrob. Chemother. Available online: http://jac.oxfordjournals.org/
145. **Harrison-Balestra C, Cazzaniga AL, Davis SC, Mertz PM.** 2003. A wound-isolated *Pseudomonas aeruginosa* grows a biofilm *in vitro* within 10 h and is visualized by light microscopy. Dermatol Surg. **29(6):**631-5.
146. **Ritger PL, Peppas NA.** 1987. A simple equation for description of solute release II. Fickian and anomalous release from swellable devices. J. Controlled Release. **5:**37-42.
147. **Peppas NA, Keys KB, Torres-Lugo M, Lowman AM.** 1999. Poly(ethylene glycol)-containing hydrogels in drug delivery. J. Controlled Release. **62:**81-7.
148. **Gong CY, Dong PW, Shi S, Fu SZ, Yang JL, Guo G, Zhao X, Wei YQ, Qian ZY.** 2009. Thermosensitive PEG-PCL-PEG hydrogel controlled drug delivery system: sol-gel-sol transition and in vitro drug release study. J Pharm Sci. **98(10):**3707-17.
149. **Zhang L, Jeong Y-II, Zheng S, Jang S-II, Suh H, Kang DH, Kim II.** 2013. Biocompatible and pH-sensitive PEG hydorgels with degradable phosphoester and phosphoamide linkers end-capped with amine for controlled drug delvery. Polym. Chem. **4:**1084-94.
150. **Cooper RA.** 2007. Iodine revisited. Int Wound J. **00:**1-4.
151. **Oliveria AS, Santos VLCG.** 2007. Topical iodophor use in chronic wounds: a literature review. Rev Latino-am Enfermagem. **15(4):**671-6.
152. **Leaper DJ, Durani P.** 2008. Topical antimicrobial therapy of chronic wounds healing by secondary intention using iodine products. Int Wound J. **5:**361-8.
153. **Pietsch J, Meakins JL.** 1976. Complications of povidone-iodine adsorption in topically treated burn patients. The Lancet **Feb. 7:**280-2.
154. **Slot J.** 2002. Selection of antimicrobial agents in periodontal therapy. J Periodont Res. **37:**389-98.
155. **Ning CC, Logsetty S, Ghughare S, Liu S.** 2014. Effect of hydrogel grafting, water and surfactant wetting on the adherence of PET wound dressings. Burns. doi: 10.1016/j.burns.2013.12.024. (Epub ahead of print)